

## Supporting Information

### SI Materials and Methods

**Bacterial strains, plasmids and growth conditions.** *Streptomyces* strains were cultivated on SFM, in YEME and on or in HT media and manipulated as described previously (1). Growth curves, RNA extractions, LC-MS and HPLC analysis were obtained from cultures grown in or on MP5 medium (2). *Escherichia coli* strains were cultivated in LB and SOB liquid medium (3). When needed these antibiotics were added into the cultures: ampicillin, apramycin, kanamycin, spectinomycin at 50µg/ml, chloramphenicol and nalidixic acid at 25µg/ml. For  $\lambda$  *red* genes induction, 10mM of filtered L-arabinose was added to the culture.

**DNA manipulation.** Plasmid and BAC DNA were extracted from *E. coli* by alkaline lysis method (3). Genomic DNA extraction of *Streptomyces* and pulsed-field gel electrophoresis were performed as already described (4). Southern blots were performed with a Hybond-N nylon membrane (Amersham-Pharmacia) and a vacuum transfer system (BioRad), as previously described (5). Amplification of DNA fragments by PCR was performed with *Taq* DNA polymerase (NEB) or Takara polymerase (Fermentas), according to the manufacturer's instructions. PCR products and restriction fragments were purified from agarose gel with the High Pure PCR product purification kit (Roche).

**Overexpression of the TCS.** The two component system-encoding sequence was amplified by PCR from *S. ambofaciens* ATCC23877 genomic DNA with the primers OE468-F and OE469-R (see Table S10 for sequences). The PCR conditions, the cloning steps into pIB139 and the integration of the recombinant plasmid (pOE-4689, Table S9) in *S. ambofaciens* ATCC23877 were as described for the overexpression of the LAL regulator (see Materials and Methods).

**Construction of the glycosyltransferase mutant strain.** The REDIRECT system was used to make an in-frame deletion of *samR0481* in *S. ambofaciens* ATCC/OE484 as already described for the deletion of *samR0467* (see Materials and Methods). However, in this case the *aac(3)IV + oriT* mutagenesis cassette was used as template in the PCR reaction with the primers D481-F and D481-R (Table S10) and the BAC of interest used was BBC (Table S9).

**Antimicrobial and antiproliferative tests.** The antibacterial activities of the purified stambomycin compounds were first analysed by loading a drop of compounds (mixture of stambomycin A and B or stambomycin C and D; from 1 µg up to 12.5 µg) onto a lawn of *Bacillus subtilis* ATCC6633 and *Micrococcus luteus* used as indicator strains. The IC50 and IC90 values were then determined only for

the mixture of stambomycin C/D (the most active fraction) against *Bacillus subtilis* BGSC 1A72, *Mycobacterium smegmatis* ATCC700084 and against clinical isolates of *Enterococcus faecalis* and *Staphylococcus aureus* (strains from Libragen, Toulouse, France). Analyses were also performed against Gram-negative bacteria (*Escherichia coli* and *Pseudomonas aeruginosa*, two clinical isolates from Libragen), against yeast (*Candida albicans* IHEM8060) and filamentous fungi (*Aspergillus fumigatus* GASP4707 and *Fusarium oxysporum* DSM2018).

For the antiproliferative activities and cytotoxicity, the IC<sub>50</sub> values were determined for stambomycin A/B and stambomycin C/D using human adenocarcinoma (HT29), breast (MCF7), lung (H460) and prostate (PC3) cancer cell lines and ovary sane cell line from an adult Chinese hamster (CHO-K1), respectively. The cell viability was determined by measuring the cellular concentration of ATP using the CellTiter-Glo® Luminescent Cell Viability Assay (Promega, G7573) according to the recommendation of the manufacturer.

#### **Identification of stambomycins by LC-MS comparative metabolic profiling.**

*Streptomyces ambofaciens* ATCC23877, ATCC/OE484 and ATCC/OE484/Δ467 spores were stored in 25% (v/v) aqueous glycerol at -20 °C. 10µl of spores from the stocks of the ATCC23877, ATCC/OE484 and ATCC/OE484/Δ467 strains were used separately to inoculate MP5 liquid medium and the resulting cultures were grown for 3-4 days at 30 °C and 180 rpm. The cultures were centrifuged for 10 minutes at 4000 rpm and 4°C. The mycelia were collected, extracted with 5 ml of methanol and sonicated for 10 minutes. The resulting suspension was filtered through a spin filter (0.4 µm) and the filtrate was analysed by LC-ESI-TOF-MS. A Sigma Ascentis C18 column (100 x 2.1mm, 2.7 µm) connected to Dionex 3000 RS-HPLC coupled with a Bruker MaXis UHR-Q-TOF mass spectrometer was used. The flow rate was 0.2 ml/min. Water/0.1% formic acid (solvent A) and methanol/0.1% formic acid (solvent B) were used as mobile phases. The elution profile was: 80% solvent A/20% solvent B for 5 minutes, gradient to 100% solvent B for 10 minutes, 100% solvent B for 5 minutes, equilibrate back to 80% solvent A/20% solvent B. The mass spectrometer was calibrated at the beginning of each run with 10 mM sodium formate and the following settings in positive ESI mode were used. Full scan: 50-2000 m/z, End plate offset: -500 V, Capillary: -4500 V, Nebulizer gas (N<sub>2</sub>): 1.6 bar, Dry gas (N<sub>2</sub>): 8 L/min, Dry Temperature: 180 °C.

ORF	Product size (aa)	% identity / similarity	Species	Putative function	Proposed role
<i>samR0465</i>	8154			Type I modular PKS	Polyketide biosynthesis
<i>samR0466</i>	3661			Type I modular PKS	Polyketide biosynthesis
<i>samR0467</i>	5771			Type I modular PKS	Polyketide biosynthesis
<i>samR0468</i>	217	84/88	<i>S. griseus</i> (SGR874)	Response regulator	Regulation
<i>samR0469</i>	442	77/84	<i>S. griseus</i> (SGR875)	Histidine kinase	Regulation
<i>samR0470</i>	261	87/93	<i>S. griseus</i> (SGR876)	Putative permease protein	Resistance
<i>samR0471</i>	312	88/93	<i>S. griseus</i> (SGR877)	Putative ABC transporter ATP-binding protein	Resistance
<i>samR0472</i>	244	55/68	<i>S. erythraea</i>	N-dimethyltransferase	D-Mycaminose biosynthesis
<i>samR0473</i>	185	46/59	<i>S. fradiae</i>	Isomerase	D-Mycaminose biosynthesis
<i>samR0474</i>	6333			Type I modular PKS	Polyketide biosynthesis
<i>samRCDS1</i>	3556			Type I modular PKS	Polyketide biosynthesis
<i>samR0475</i>	3157			Type I modular PKS	Polyketide biosynthesis
<i>samR0476</i>	3565			Type I modular PKS	Polyketide biosynthesis
<i>samRCDS2</i>	1569			Type I modular PKS	Polyketide biosynthesis
<i>samR0477</i>	5447			Type I modular PKS	Polyketide biosynthesis
<i>samR0478</i>	414	43/62	<i>S. fradiae</i>	Cytochrome P450	Polyketide hydroxylation
<i>samR0479</i>	401	41/56	<i>R. castenholzii</i>	Cytochrome P450	Polyketide hydroxylation
<i>samR0480</i>	369	74/82	<i>Streptomyces</i> sp. TP-A0274	Aminotransferase	D-Mycaminose biosynthesis
<i>samR0481</i>	418	48/63	<i>M. griseorubida</i>	Glycosyltransferase	D-Mycaminose attachment
<i>samR0482</i>	595	64/75	<i>S. hygrosopicus</i>	Acyl-CoA synthetase	Unknown
<i>samR0483</i>	532	62/75	<i>Micromonospora</i> sp. ATCC39149	Carboxyl transferase	Precursor biosynthesis
<i>samR0484</i>	958	35/47	<i>S. venezuelae</i> (PikD)	Transcriptional activator (LAL)	Regulation
<i>samR0485</i>	255	87/94	<i>S. griseus</i> (SGR200)	Type II thioesterase	PKS editing
<i>samR0486</i>	329	77/84	<i>S. tenebrarius</i> (AprE)	dTDP-glucose-4,6- dehydratase	D-Mycaminose biosynthesis
<i>samR0487</i>	290	74/85	<i>S. avermitilis</i> (AveBIII)	Glucose-1-phosphate thymidyltransferase	D-Mycaminose biosynthesis

**Table S1.** Properties of genes within the stambomycin biosynthetic cluster. Putative functions of the encoded proteins were deduced from analyses with the BlastP program (<http://blast.ncbi.nlm.nih.gov/Blast.cgi>). The % identity/similarity for the protein in the database with the highest end-to-end similarity is indicated. The stambomycin cluster is located in the right terminal region of the chromosome which has been fully sequenced (AM238664).

	*	*	*****	*	**	*
AT1	AMIFSGQGS-53-VVQPA-22-VA	GHSQGEI-18-VALRS-70-PVDYAS	SHSAHVE-45-LRSTVEFSA			
AT2	GFLFTGQGS-50-YAQAG-22-LV	GHSIGEL-18-VSARG-66-AVSHA	FHSRLME-40-IREPVRFAD			
AT3	GFLFTGQGS-50-YAQAG-22-LV	GHSVGEI-18-VSARG-66-AVSHA	FHSRLME-40-VREPVRFAD			
AT4	ALLFSGQGS-50-YAQAG-22-LV	GHSIGEL-18-VSARG-66-AVSHA	FHSRLME-40-VREPVRFAD			
AT5	ALLFSGQGA-50-YTQPA-22-LV	GHSIGEL-18-VSARA-66-AVSHA	FHSRLME-40-IVAPVRFAD			
AT6	VFVFPQGS-52-VVQPV-22-VV	GHSQGEI-18-VALRS-71-PVDYAS	SHSVQVE-45-LRSTVRFEE			
AT7	GFLFTGQGA-51-WTQAG-22-LL	GHSIGEV-18-VEARG-68-TVSHA	FHSALME-46-VRQAVRFAD			
AT8	VFVFPQGS-52-VVQPV-22-VV	GHSQGEI-18-VALRS-71-PVDYAS	SHSVQVE-45-LRSTVRFEE			
AT9	AFLFTGQGA-50-WTQAG-22-LL	GHSIGEI-18-VAARG-68-TVSHA	FHSALME-41-VRETVRFAD			
AT10	AFLFTGQGA-50-WAQAG-22-LL	GHSIGEI-18-VAQRG-68-TVSHA	FHSALME-41-VRETVRFAD			
AT11	AFLFTGQGA-50-WAQAG-22-LL	GHSVGEI-18-VAARG-68-TVSHA	FHSVLMME-46-VREAVRFAD			
AT12	ALLFSGQGS-50-YAQAG-22-LV	GHSIGEL-18-VSARG-66-AVSHA	FHSRLME-40-VREPVRFAD			
AT13	AFVLPQGS-53-VIQPV-22-VV	GHSQGEI-18-VTHRS-71-RIKGA	SHSAVVE-45-MRQTVQFAP			
AT14	AFVFPQGG-53-VTPVV-22-VL	GHSQGEI-18-VALRG-71-RVDFS	SHCAQVE-45-LVTPVDLDR			
AT15	ALLFSGQGS-50-YAQAG-22-LV	GHSVGEI-18-VSARG-66-AVSHA	FHSRLME-40-VREPVRFAD			
AT16	ALLFSGQGS-50-YAQAG-22-LV	GHSIGEL-18-VSARG-66-AVSHA	FHSRLME-40-VREPVRFAD			
AT17	ALLFSGQGS-50-YAQAG-22-LV	GHSVGEI-18-VSARG-66-AVSHA	FHSRRMD-40-VREPVRFAD			
AT18	VFVFPQGS-53-VVQPV-22-VV	GHSQGEI-18-VALRA-71-PVDYAS	SHCAQVE-45-LRNTVRFEE			
AT19	ALLFSGQGS-50-YAQAG-22-LV	GHSIGEL-18-VSARG-66-AVSHA	FHSHLME-40-VREPVRFAD			
AT20	AFLFTGQGA-49-HTQPA-22-LA	GHSIGEL-18-VAARG-66-AVSHA	FHSHLME-42-VRSTVRFAG			
AT21	VFVFPQGS-51-VVQPV-22-VV	GHSQGEI-18-VALRA-71-PVDYAS	SHCAQVE-45-LRNTVRFEE			
AT22	VFVFPQGS-51-VVQPV-22-VV	GHSQGEI-18-VALRA-71-PVDYAS	SHCAQVE-45-LRNTVRFEE			
AT23	ALLFSGQGS-50-YAQAG-22-LV	GHSQGEI-18-VSARG-66-AVSHA	FHSRLME-40-VREPVRFAD			
AT24	VFVFPQGS-51-VVQPV-22-VV	GHSQGEI-18-VALRA-71-PVDYAS	SHSAHVE-45-LRATVRFED			
AT25	AFVFSQGA-51-WTQLG-22-LA	GHSVGEV-18-VAARG-71-DVSHA	FHSRVD-45-IRATVRFAD			
	Q	Q	GH[LVI]FAM[G	R	[FP]H	V malonyl-CoA
	Q	Q	GH[QMI]G	R	SH	V methylmalonyl-CoA

**Fig. S1.** Sequence alignment of the PKS AT domains. Highly conserved active site residues are marked with an asterisk (\*). The boxed residues are diagnostic of substrate specificity, in particular the amino acid underlined in green. The arginine residue underlined in yellow interacts with the carboxyl group of the substrates. The catalytic serine residue is underlined in blue. The consensus sequences for malonyl-CoA and methylmalonyl-CoA-specific AT domains are shown below the alignment. The substrate for AT13 could not be predicted because the circled specificity-conferring residue is different from that found in malonyl- and methylmalonyl-CoA-specific AT domains.

		↓	↓	
<b>KR2</b>	PHDTVLI TGGT GALGARVARHLVCA-57-VVHTAGVLD DGLL TSLTPE-26-FVLFSSVAASF GTAGQAS YAAANAF LD			B1
<b>KR3</b>	-DGTVLVTGGT GALGAQVAR-LLAA-61-VVHAAGVLD DGV IDGLTPE-26-FVLFSSFTGAVGTAGQANYAAANAHLD			B1
<b>KR4</b>	--GTVLVTGGT GALGAHTARLLARR-60-VVHAAGTVDDGVIGSLTPG-26-FVLYTSFAGVVG NLGQAA YAAAGNAALD			B1
<b>KR5</b>	PQGT VLI TGGT GTLGS LLARHLVEH-62-VVHAAGVADDGVIEAL TPE-26-FTVYASASSAF GSPGQANYAAANAF LE			B1
<b>KR6</b>	--GTVLVTGGT GAVGA EVARWLAGR-60-VLHAAGVDVGTALDEVDAD-26-FVVFSSGAAVWGGGQQA YAAAGNAFLD			A1
<b>KR7</b>	--GTVLVTGGT GGLGGEVARWLARR-60-VVHAAGVGT PGRLLD TDET-24-FVVFSSIAATW GSGGQQA YAAAGNAFLD			A1
<b>KR8</b>	PDGT VLI TGGT GTLGG LLARHLVTE-62-VIHAAGVLD DGVFESMTPE-26-FVLYSSASATL GTGGQANYAAANSFLD			B1
<b>KR9</b>	--GTVLVTGGT GALGKRVARWLAER-60-VVHAAGVGGQAVPLADTDEA-26-FVVFSSIAATW GSGGQQA YAAANAHLD			A1
<b>KR10</b>	-PGAVLVTGGT GALGAVVARWLADR-60-VVHAAGVLD DGTLDAL TPE-26-FVAFSSLAGTVGSAGQGN YAAANAFVD			B1
<b>KR11</b>	-PGTVLVTGGT GALGASVARWLAER-60-VVHAAGVAQSGPVETTRLA-26-FVLFSSIAATW GSGGQAL YAAAGNAYLD			A1
<b>KR12</b>	AEGTVLVTGGT GALGALTARHLVVE-62-VVHAAGI LD DGLVESL TED-25-FVMYSSMSGTF GSPGQQA YAAANAYLD			B1
<b>KR13</b>	--STVLI TGGTGGI GRHLAHHMAAR-56-VIHAAGVAQAT ALADCGES-24-FVLFSSGAGVWGGAGQA YAAAGNAVLD			A1
<b>KR14</b>	ADGT VLV T GATG T LGSALARHLVRH-61-VVHTAAVLD DGVLAQMTDR-26-FALFSSAAGVLGGAGQANYAAANVFLD			B1
<b>KR15</b>	--GTVLI TGGT GALGSRVARWAALA-56-VVHAAGVGG LGRLAE LTEE-24-FVLFGSVAAVWGGAGQA YAAANARLE			A1
<b>KR16</b>	--GTVLVTGGT GALGAHVARWLADR-56-VVHAAGSGGFGTLD DASEA-26-FVLFSSVSGI WSGGQQA YGAANAALD			A1
<b>KR17</b>	PGGT VLI TGGT GALGALVARYLVDR-44-VFHLAGVLD DGVATAL TPE-24-FVLFSSVSATL GSPGQAS YAAANAYLD			B1
<b>KR18</b>	--EAVLI TGGT GALGAETARMLARR-56-VVHAAGTDPAL PLDSTV P-24-FVVFSSIAGVW GSGGQQA YAAANAHLD			A1
<b>KR19</b>	--GTVLVTGGT GAI GGHVARWLATE-62-VMHTAGLGV LADTGV A-26-VVHFSSIAAMWGVGGHQG YAAGNAYLD			A2
<b>KR20</b>	AHGT VLV TGGT GVLGGRVARHLAAR-62-VVHAAGIVDDGVV TSLTPD-24-FVLFSSASATF GSAGQAGYAAANAVLD			B1
<b>KR21</b>	PVGT VLV TGGT GVLGGLVARHLVTA-57-VVHAAGVLD DGVFESMTPK-23-FVVFSSAGGTF GPAGQANYAAANATLD			B1
<b>KR22</b>	--GTVLVTGGT GGI GAHVARWLAAS-61-VFHAAGIVDSS ILLD SLTPD-26-FVLFSSLAGVFGSAGEGNYAPGN AFLD			B2
<b>KR23</b>	-P--VLLTGGT GALGGKVARLLAER-56-VVHAAGIVDDGVLDAL TPE-24-FVVFSSVAGVIGSAGQGP YAAANAHLD			B1
<b>KR24</b>	--GPVLVTGGT GALGREVARWLARR-56-VVHTAGISTTAPLAGTSPA-25-FVLFSSIAGVWGGGQQA YAAANAHLD			A1
<b>KR25</b>	--GTVLITGGT GRRGRALATALAAN-55-VVHAVGAGEDTPWTE LSPG-26-FVLVSSVTGVWGGTGA AVRAAASARMD			C1
Cons	GXGXXGXXXX	*	*	*

**Fig. S2.** Sequence alignment of the PKS KR domains. The GXGXXGXXXX consensus sequence in the N-termini is proposed to bind NAD(P)H (7). The residues belonging to the catalytic triad are marked with asterisks. The Y to R and N to S mutations of the catalytic residues in KR25 indicate that it is not active. The arrows indicate the residue predictive of B and A-type alcohol stereochemistry, respectively. The predicted configurations of the  $\alpha$ - and  $\beta$ -stereocenters generated by each KR, according to the model of Keatinge-Clay (8), are indicated to the right of the alignment. A1 = 2R, 3S; A2 = 2S, 3S; B1 = 2R, 3R; B2 = 2S, 3R; C1 = 2R.

ER11	VNFRDVLNVLGMYPG-EVLVGGEAAGVV-67-SAGESVLVHAAAGGVGMAAVQVARHLG
ER16	MNFRDVLNVLGMYPG-EVELGGEAAGVV-67-AAGESVLVHAAAGGVGMAAVQIARHVG
ER4	VNFRDVLIALGQYDPDTALMGSEAAGVV-67-SAGESVLVHAAAGGVGMAAVQVARHLG
ER7	VNFRDVLIALGMPD-RAQMGAEAAGVV-67-RPGESVLVHSAAGGVGMAAVQLGRHLG
	:***** .** ** . :.****** .*****:*****:*****:***:

**Fig. S3.** Sequence alignment of the PKS ER domains. The highly conserved putative NADPH binding motif is highlighted in yellow. The residue that is predictive of stereochemistry is highlighted in red. A tyrosine residue in this position predicts the 2S configuration. Another residue (usually Val or Ala) in this position predicts the 2R stereochemistry (9).

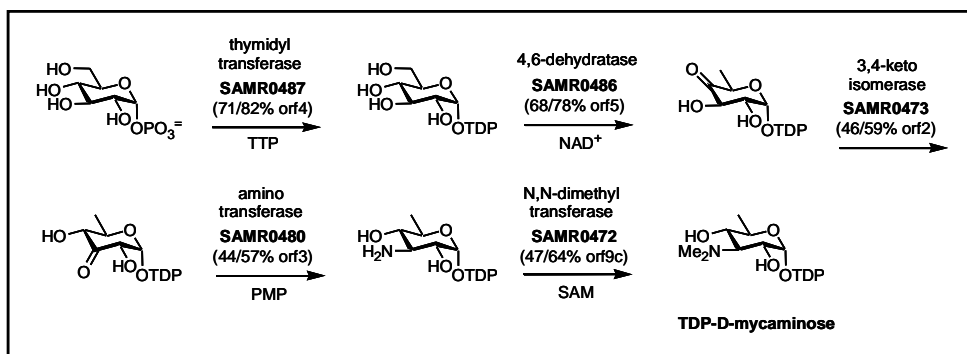


**Fig. S4.** TDP-D-mycaminose biosynthetic pathway. Proposed pathway for biosynthesis of TDP-D-mycaminose from  $\alpha$ -D-glucose-1-phosphate by putative aminodeoxysugar biosynthetic enzymes encoded by genes within the cluster. For each enzymatic step, the gene product is indicated in bold. The identity/similarity with the corresponding enzymes involved the biosynthesis of the  $\beta$ -D-mycaminose residue of spiramycin are indicated in brackets (10). TTP, thymidine triphosphate; TDP, thymidine diphosphate;  $\text{NAD}^+$ , nicotinamide adenine dinucleotide; PMP, pyridoxamine 5'-phosphate; SAM, S-adenosyl-L-methionine.

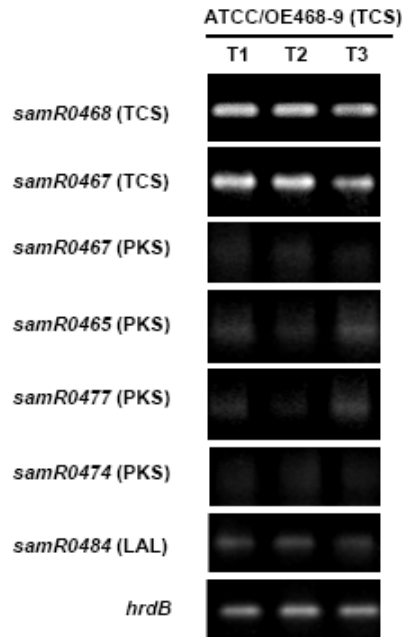


**Fig. S5.** Transcriptional analysis of the strain overexpressing the two component system (mutant strain ATCC/OE468-9) and grown in MP5 medium. The expression of four biosynthetic genes (*samR0467*, *samR0465*, *samR0477*, *samR0474*), together with the expression of the regulatory genes *samR0468*, *samR0469* and *samR0484*, were analyzed by RT-PCR using 4 $\mu$ g of total RNA. The constitutively-expressed *hrdB* gene, coding for the major sigma factor, was used as a positive control. Experiments carried out on three separate occasions gave the same result. T1= exponential phase; T2= transition phase; T3= stationary phase.

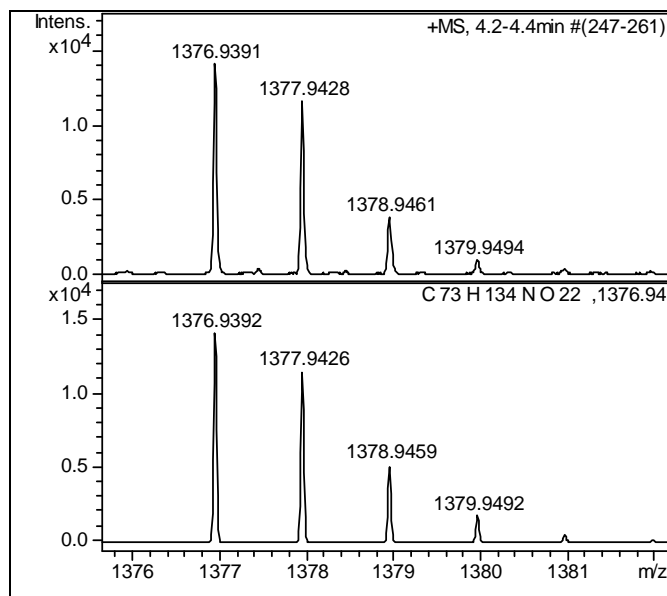


**Fig. S6.** High resolution mass spectrometry analysis of stambomycins A/B. Measured spectrum of stambomycins A/B (top panel) and simulated spectrum for  $C_{73}H_{134}NO_{22}^+$  (bottom panel).

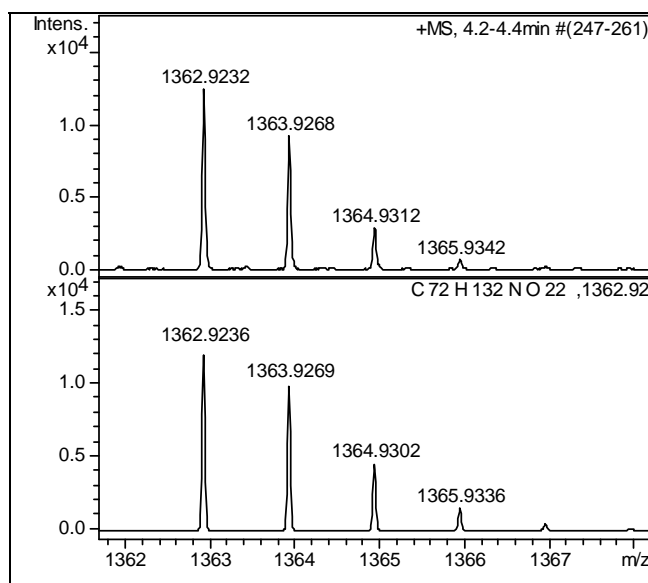


**Fig. S7.** High resolution mass spectrometry analysis of stambomycins C/D. Measured spectrum of stambomycins C/D (top panel) and simulated spectrum for  $C_{72}H_{132}NO_{22}^+$  (bottom panel).



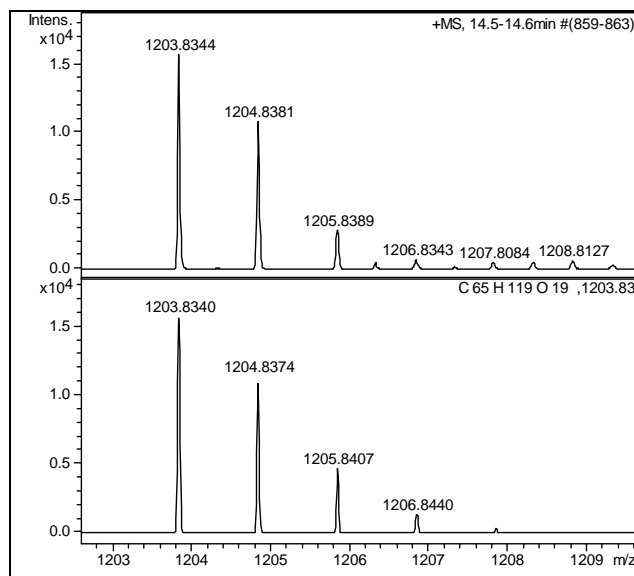


**Fig. S8.** High resolution mass spectrometry analysis of stambomycin A/B aglycones. Measured spectrum of stambomycin A/B aglycones (top panel) and simulated spectrum for C<sub>65</sub>H<sub>119</sub>O<sub>19</sub><sup>+</sup> (bottom panel).

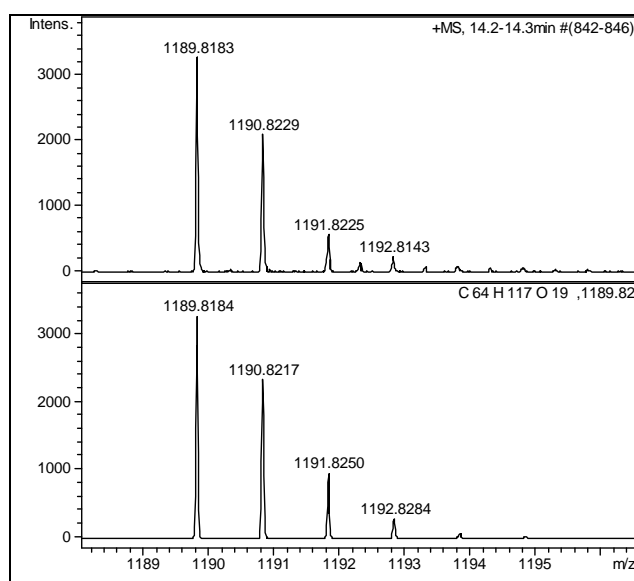


**Fig. S9.** High resolution mass spectrometry analysis of stambomycin C/D aglycones. Measured spectrum of stambomycin C/D aglycones (top panel) and simulated spectrum for C<sub>64</sub>H<sub>117</sub>O<sub>19</sub><sup>+</sup> (bottom panel).



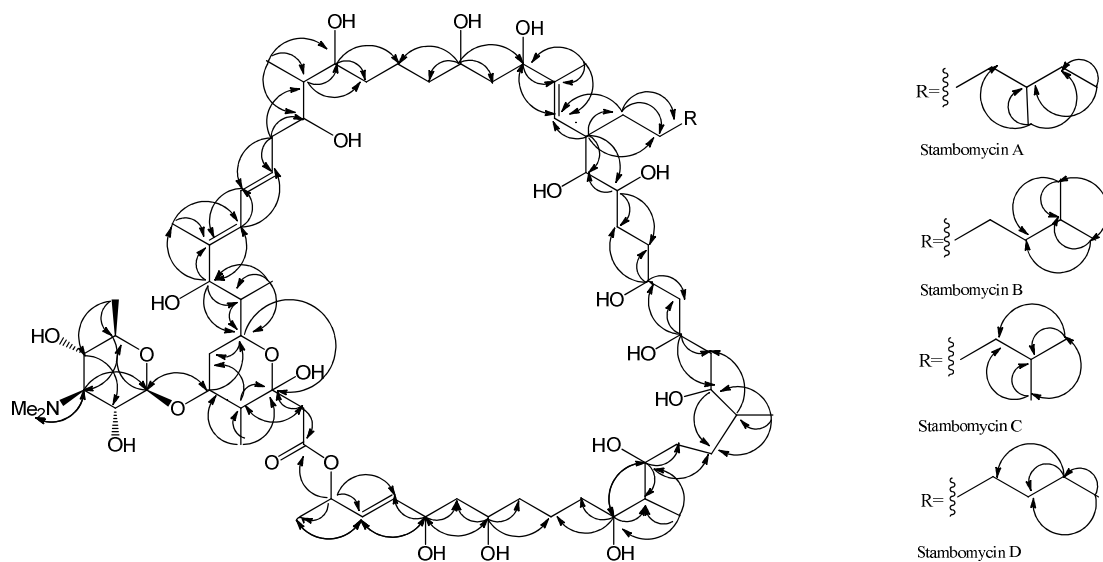


**Fig. S12.** Summary of HMBC NMR correlations observed for stambomycins A-D in  $d_4$ -MeOH.

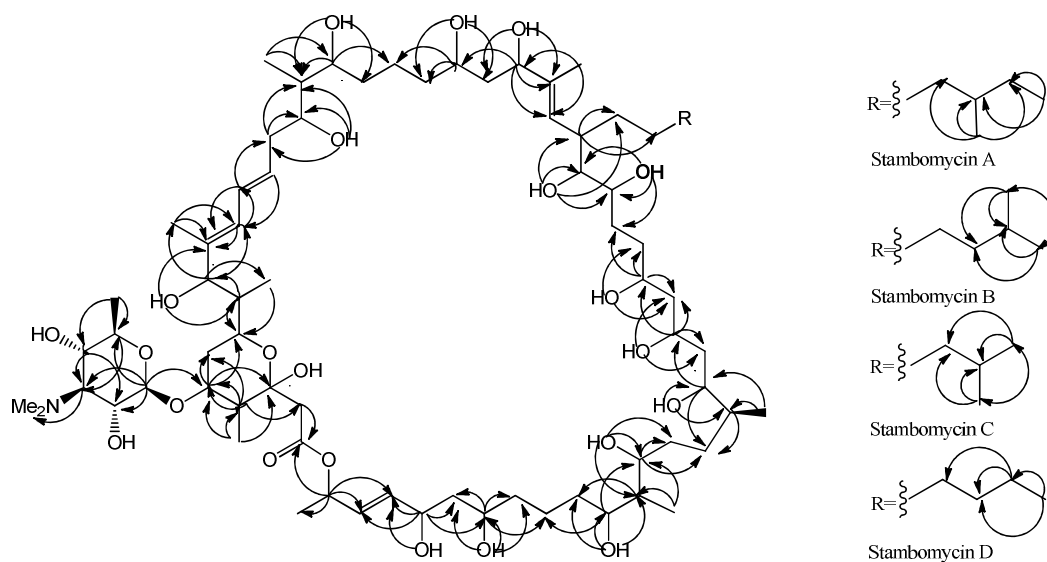


**Fig. S13.** Summary of HMBC NMR correlations observed for stambomycins A-D in  $d_6$ -DMSO.

**Table S2.** Assignments of  $^1\text{H}$  and  $^{13}\text{C}$  NMR signals for stambomycins A and B. Carbon atom numbering is shown in Fig. S10. Signals for C-1'' to C-7'' of stambomycin B are in brackets.

position	$\delta_{\text{C}}$ (ppm)	$\delta_{\text{H}}$ (ppm)	$J_{\text{H-H}}$ (Hz)
1	173.3		
2	44.3	2.52, 2.83	15.0
3	100.0		
4	46.2	1.56	
4-Me	12.4	1.04	
5	81.0	3.66	
1'	104.6	4.44	7.3
2'	70.0	3.54	7.3, 10.5
3'	72.0	3.23	10.5, 10.5
4'	70.8	3.38	9.8, 10.5
5'	74.0	3.42	9.8, 6.2
6'	18.1	1.29	
3'-NMe <sub>2</sub>	42.2	3.03	
6	39.1	1.61, 1.90	
7	70.0	3.83	
8	40.8	1.56	
8-Me	9.3	0.93	
9	79.9	3.90	7.6
10	137.1		
10-Me	12.4	1.65	
11	128.0	6.04	11.0
12	129.9	6.35	15.0, 11.0
13	131.7	5.80	15.0, 6.9
14	39.8	2.34	6.9
15	75.8	3.77	
16	42.6	1.52	
16-Me	7.4	0.94	
17	75.5	3.72	
18	36.1	1.48	
19	23.5	1.33, 1.34	
20	38.6	1.48	
21	71.1	3.55	
22	43.1	1.61, 1.67	
23	77.5	4.23	7.0
24	139.2		
24-Me	12.2	1.64	
25	129.3	5.23	10.5
26	41.9	2.45	
1''	32.9 (32.5)	1.19, 1.77 (1.19, 1.78)	
2''	25.7 (26.6)	1.35 (1.42)	
3''	38.3 (31.8)	1.13, 1.29 (1.29)	
4''	35.7 (40.2)	1.30 (1.19, 1.50)	
5''	30.8 (29.1)	1.13 (1.30)	
6''	12.1 (23.0)	0.86 (0.87)	
7''	19.6 (23.0)	0.85 (0.87)	
27	79.7	3.36	
28	74.2	3.47	
29	27.8	1.43, 1.68	
30	36.1	1.43, 1.70	
31	70.1	3.83	
32	46.4	1.50, 1.57	
33	66.8	4.06	
34	42.0	1.48, 1.50	
35	72.9	3.74	

36	40.8	1.48	
36-Me	15.6	0.92	
37	29.8	1.28, 1.11	
38	36.0	1.50	
39	76.3	3.72	
40	42.3	1.51	
40-Me	7.0	0.91	
41	75.9	3.71	
42	33.8	1.43, 1.62	
43	22.9	1.43	
44	38.8	1.45, 1.46	
45	70.6	3.67	
46	44.8	1.60, 1.65	
47	71.1	4.28	6.3, 12.9
48	136.7	5.80	15.3, 6.3
49	130.8	5.72	6.3, 15.3
50	72.8	5.43	6.3,
51	20.8	1.33	6.3

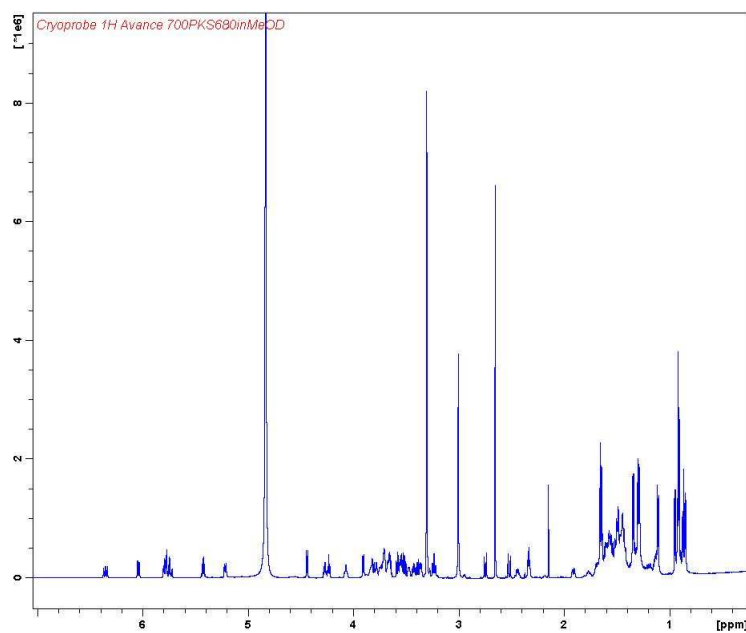


**Fig. S14.** <sup>1</sup>H NMR spectrum (700 MHz, d<sub>4</sub>-MeOH) of stambomycins A/B.

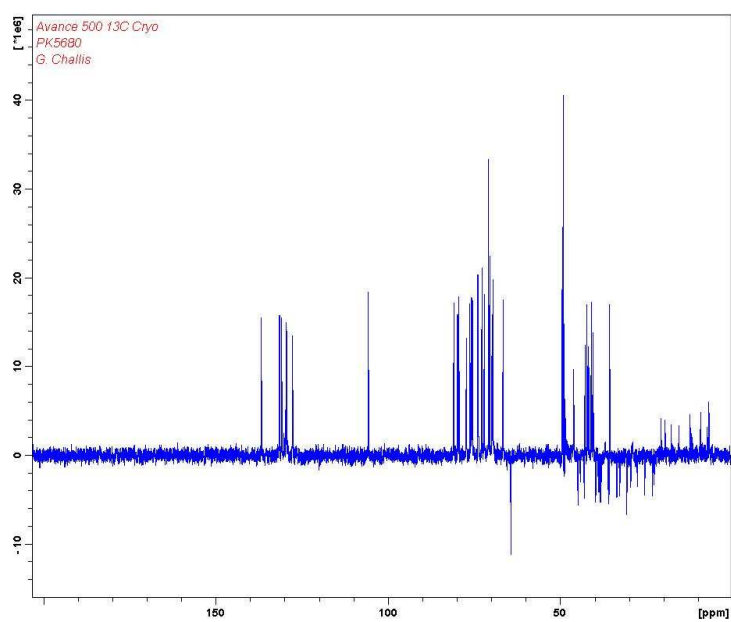


**Fig. S15.**  $^{13}\text{C}$  PENDANT NMR spectrum (125 MHz,  $d_4$ -MeOH) of stambomycins A/B.

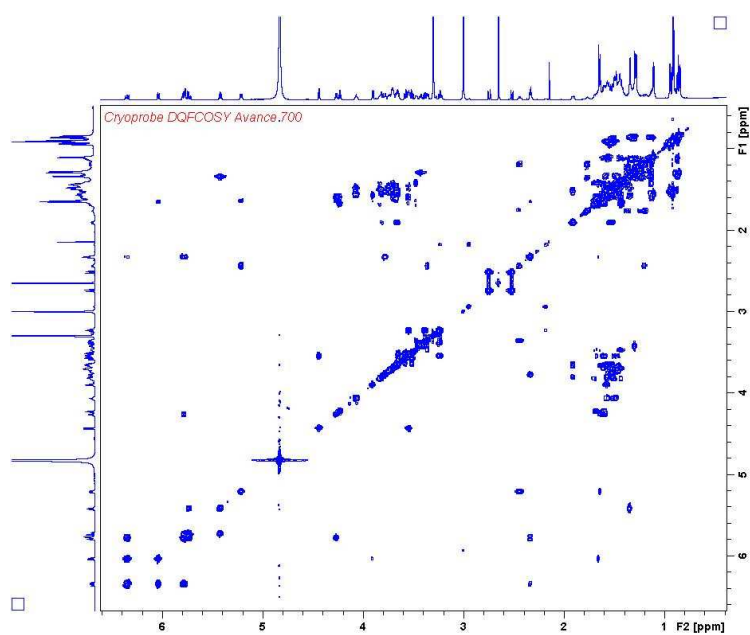


**Fig. S16.** DQFCOSY NMR spectrum (700 MHz,  $d_4$ -MeOH) of stambomycins A/B.

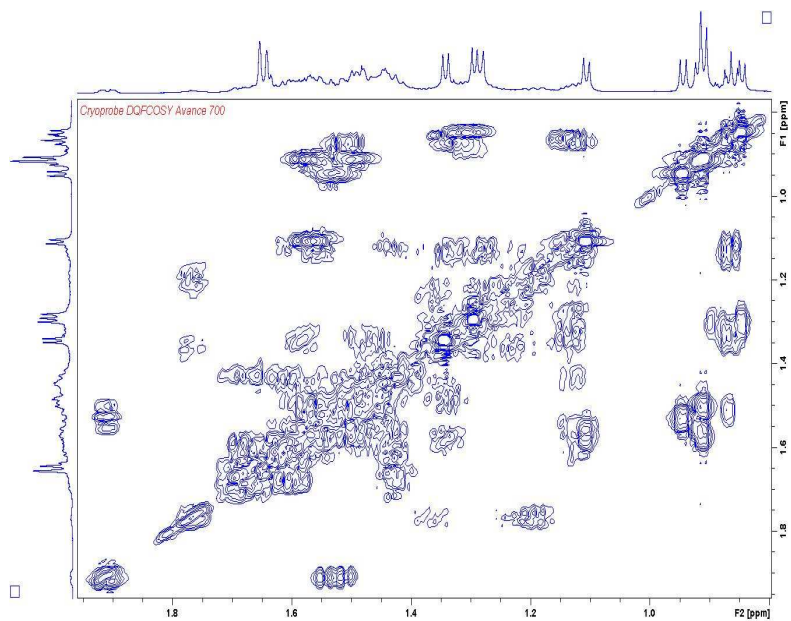


**Fig. S17.** Expansion of methyl/methylene region of DQFCOSY spectrum of stambomycins A/B.

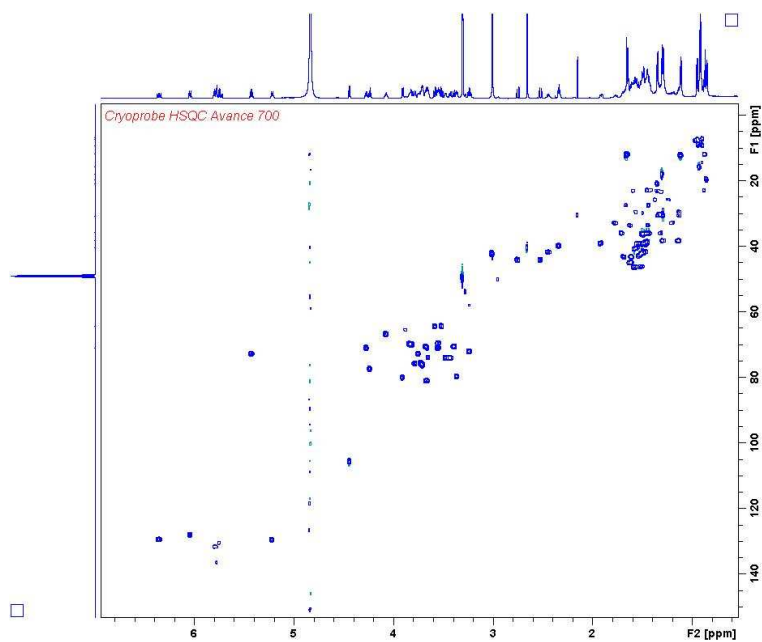


**Fig. S18.** HSQC NMR spectrum (700 MHz/175 MHz, d<sub>4</sub>-MeOH) of stambomycins A/B.

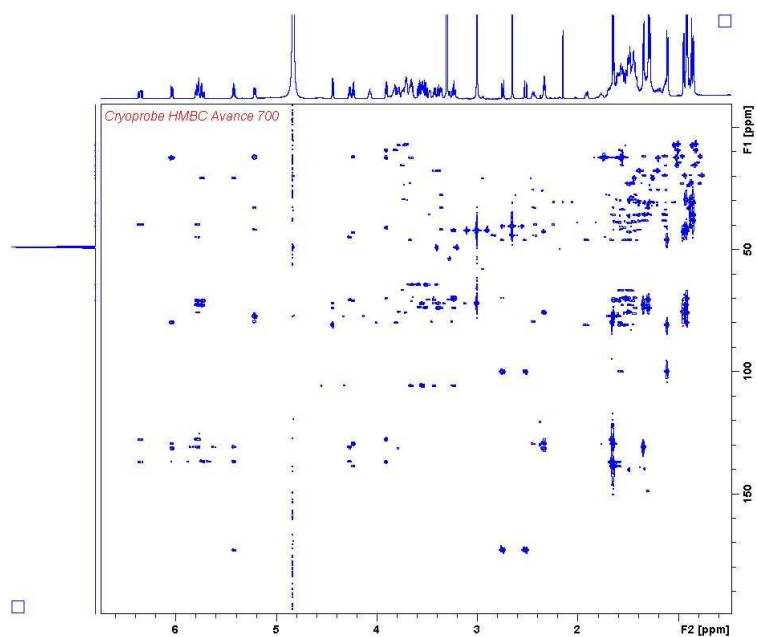


**Fig. S19.** HMBC NMR spectrum (700 MHz/175 MHz, d<sub>4</sub>-MeOH) of stambomycins A/B.

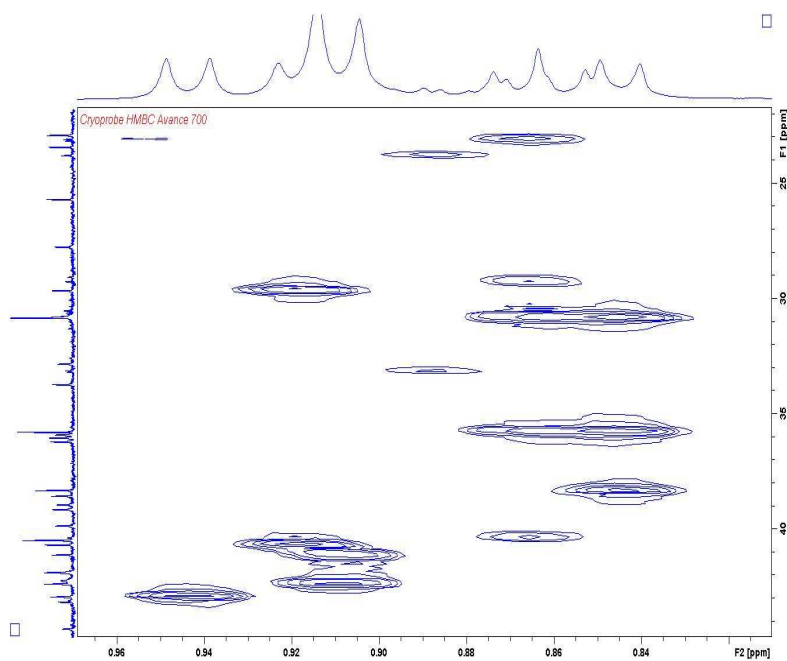


**Fig. S20.** Expansion of methyl region of HMBC spectrum of stambomycins A/B.



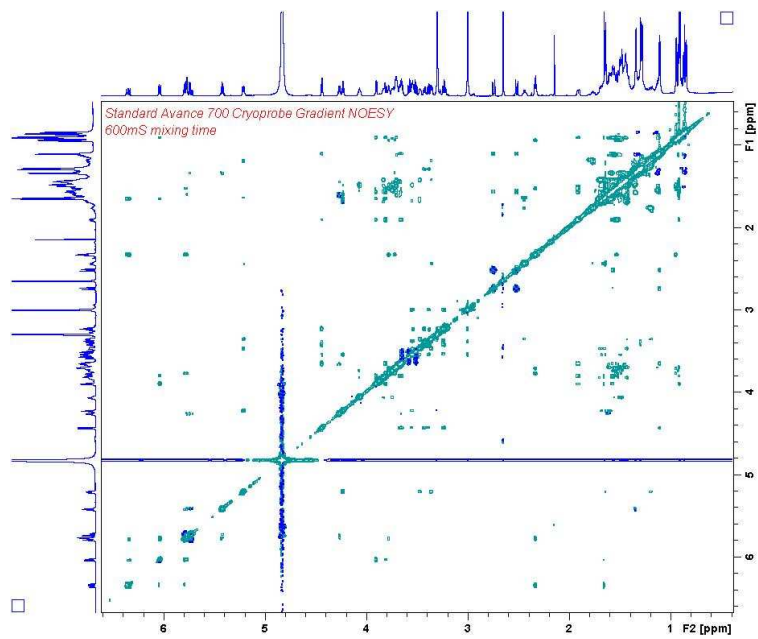


**Fig. S21.** NOESY NMR spectrum (700 MHz, d<sub>4</sub>-MeOH) of stambomycins A/B.

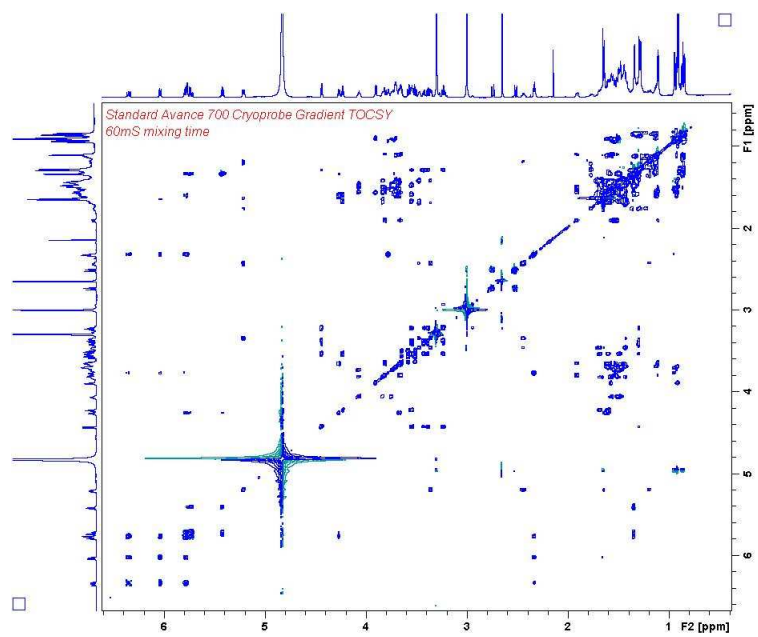


**Fig. S22.** TOCSY NMR spectrum (700 MHz, d<sub>4</sub>-MeOH) of stambomycins A/B.

**Table S3.** Assignments of  $^1\text{H}$  and  $^{13}\text{C}$  NMR signals for stambomycins C/D. Carbon atom numbering is shown in Fig. S10. Signals for C-1'' to C-6'' of stambomycin D are in brackets.

position	$\delta_{\text{C}}$ (ppm)	$\delta_{\text{H}}$ (ppm)	$J_{\text{H-H}}$ (Hz)
1	173.3		
2	44.3	2.52, 2.83	15.0
3	100.0		
4	46.2	1.56	
4-Me	12.4	1.04	
5	81.0	3.66	
1'	104.6	4.44	7.3
2'	70.0	3.54	7.3, 10.5
3'	72.0	3.23	10.5, 10.5
4'	70.8	3.38	9.8, 10.5
5'	74.0	3.42	9.8, 6.2
6'	18.1	1.29	
3'-NMe <sub>2</sub>	42.2	3.03	
6	39.1	1.61, 1.90	
7	70.0	3.83	
8	40.8	1.56	
8-Me	9.3	0.93	
9	79.9	3.90	7.6
10	137.1		
10-Me	12.4	1.65	
11	128.0	6.06	11.0
12	129.9	6.35	15.0, 11.0
13	131.7	5.81	15.0, 6.9
14	39.8	2.34	6.9
15	75.8	3.77	
16	42.6	1.52	
16-Me	7.4	0.95	
17	75.5	3.72	
18	36.1	1.48	
19	23.5	1.32, 1.34	
20	38.5	1.47	
21	71.1	3.55	
22	43.1	1.61, 1.67	
23	77.5	4.23	6.9
24	139.4		
24-Me	12.2	1.64	
25	129.3	5.23	6.5
26	41.9	2.45	
1''	32.5 (32.4)	1.18, 1.79 (1.18, 1.79)	
2''	25.8 (26.6)	1.38 (1.37)	
3''	40.3 (35.8)	1.13, 1.29 (1.31, 1.44)	
4''	29.9 (34.0)	1.30 (1.43, 1.49)	
5''	23.1 (29.2)	0.87 (1.29)	
6''	23.1 (11.5)	0.87 (0.87)	
27	79.7	3.36	
28	74.2	3.47	
29	27.8	1.43, 1.68	
30	36.1	1.43, 1.70	
31	70.1	3.83	
32	46.4	1.50, 1.57	
33	66.8	4.06	
34	42.0	1.48, 1.50	

35	72.9	3.74	
36	40.8	1.48	
36-Me	15.6	0.92	
37	29.8	1.28, 1.12	
38	36.0	1.50	
39	76.3	3.72	
40	42.3	1.51	
40-Me	7.0	0.91	
41	75.9	3.71	
42	33.8	1.43, 1.62	
43	22.9	1.43	
44	38.8	1.45, 1.46	
45	70.6	3.67	
46	44.8	1.60, 1.65	
47	71.1	4.28	6.2, 12.9
48	136.7	5.80	15.0, 6.2
49	130.8	5.72	6.2, 15.0
50	72.8	5.43	6.2
51	20.8	1.33	6.2

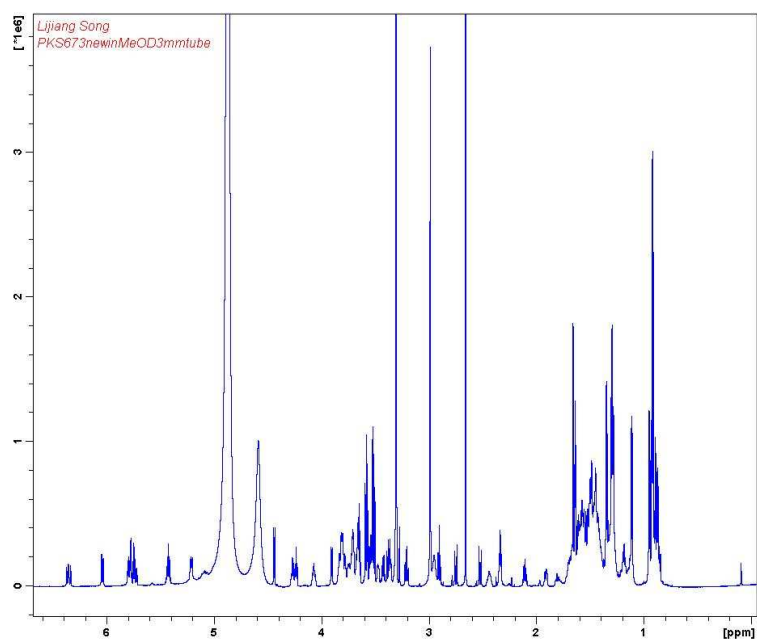


**Fig. S23.** <sup>1</sup>H NMR spectrum (700 MHz, d<sub>4</sub>-MeOH) of stambomycins C/D.

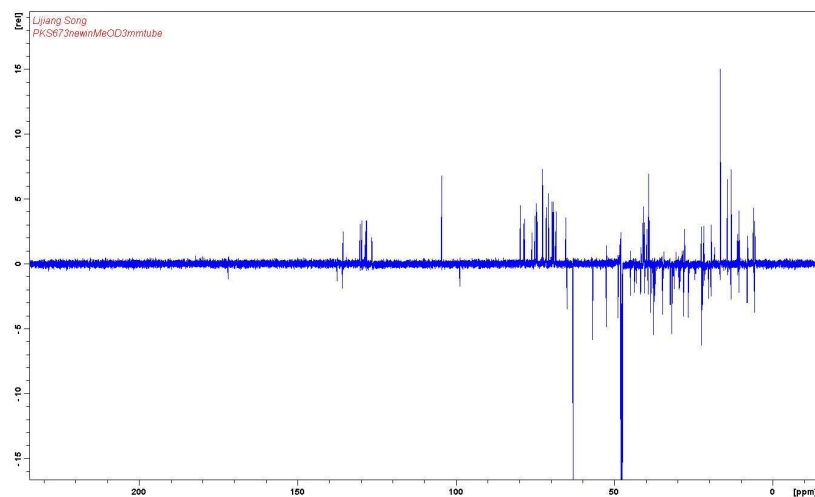


**Fig. S24.**  $^{13}\text{C}$  PENDANT NMR spectrum (175 MHz,  $\text{d}_4\text{-MeOH}$ ) of stambomycins C/D.

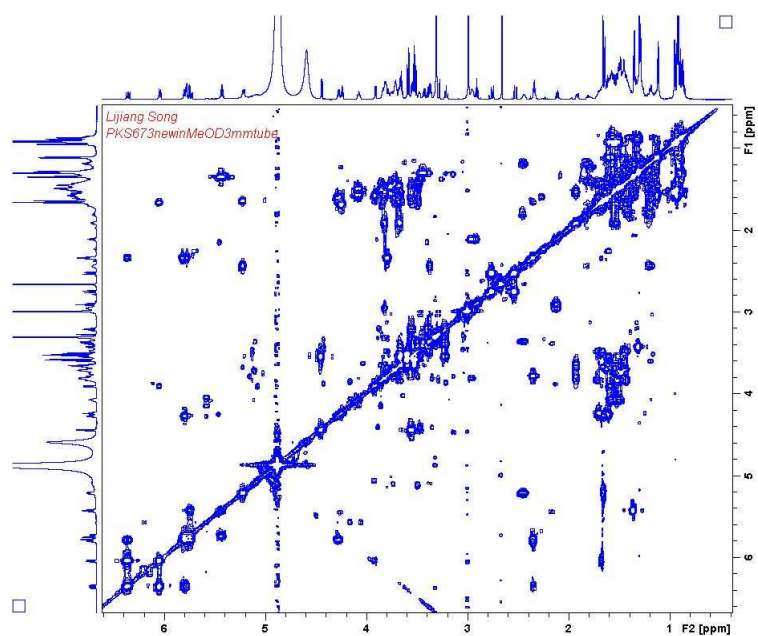


**Fig. S25.** DQFCOSY NMR spectrum (700 MHz,  $\text{d}_4\text{-MeOH}$ ) of stambomycins C/D.

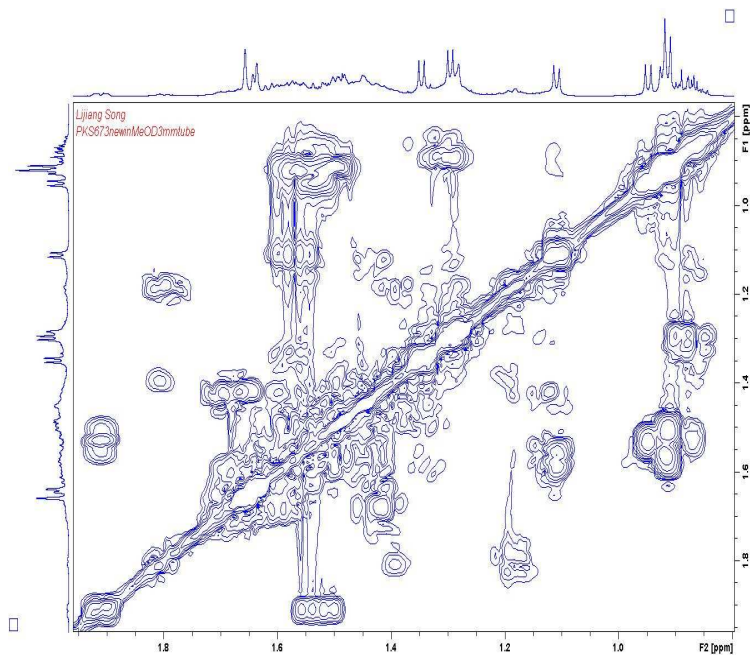


**Fig. S26.** Expansion of methyl/methylene region of DQFCOSY spectrum of stambomycins C/D.

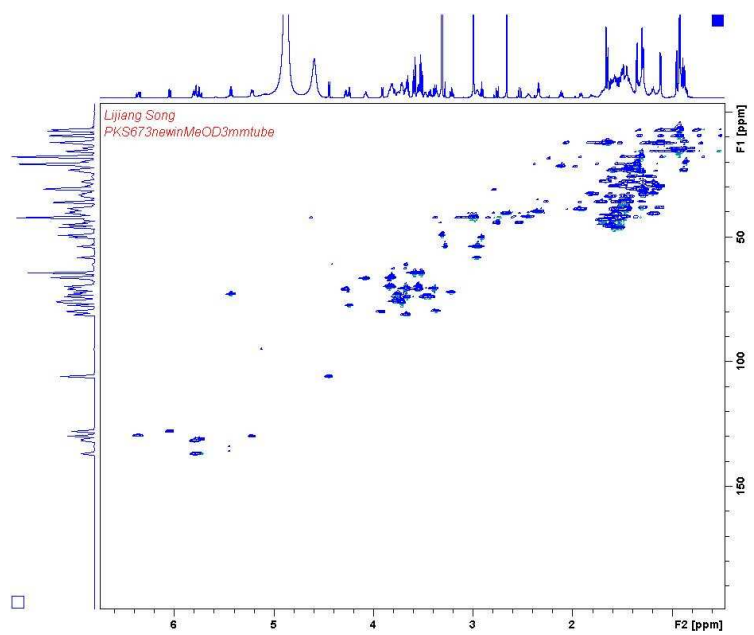


**Fig. S27.** HSQC NMR spectrum (700 MHz/175 MHz, d<sub>4</sub>-MeOH) of stambomycins C/D.

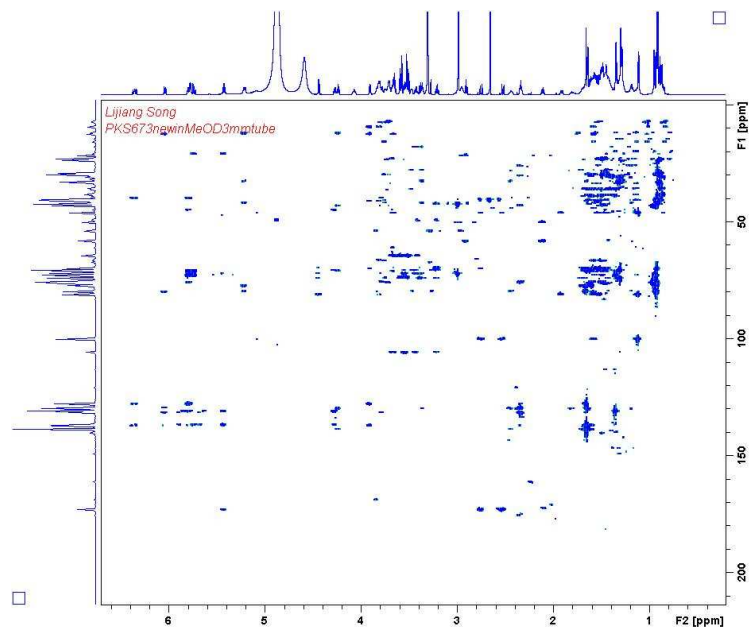


**Fig. S28.** HMBC NMR spectrum (700 MHz/175 MHz, d<sub>4</sub>-MeOH) of stambomycins C/D.

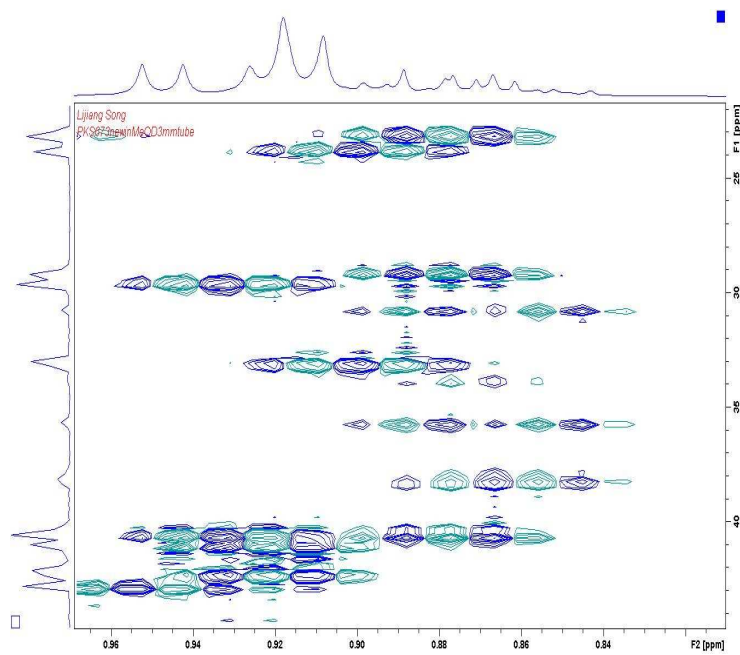


**Fig. S29.** Expansion of methyl region of HMBC spectrum of stambomycins C/D.

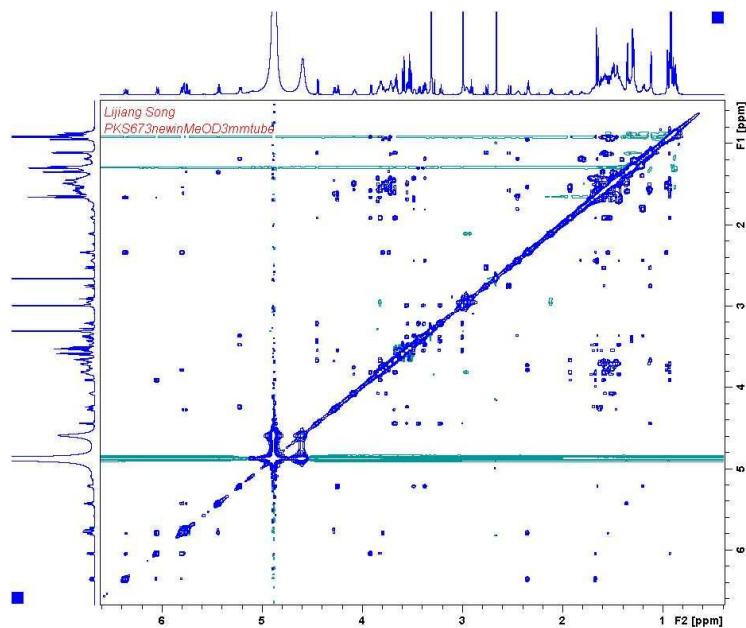


**Fig. S30.** NOESY NMR spectrum (700 MHz,  $d_4$ -MeOH) of stambomycins C/D.

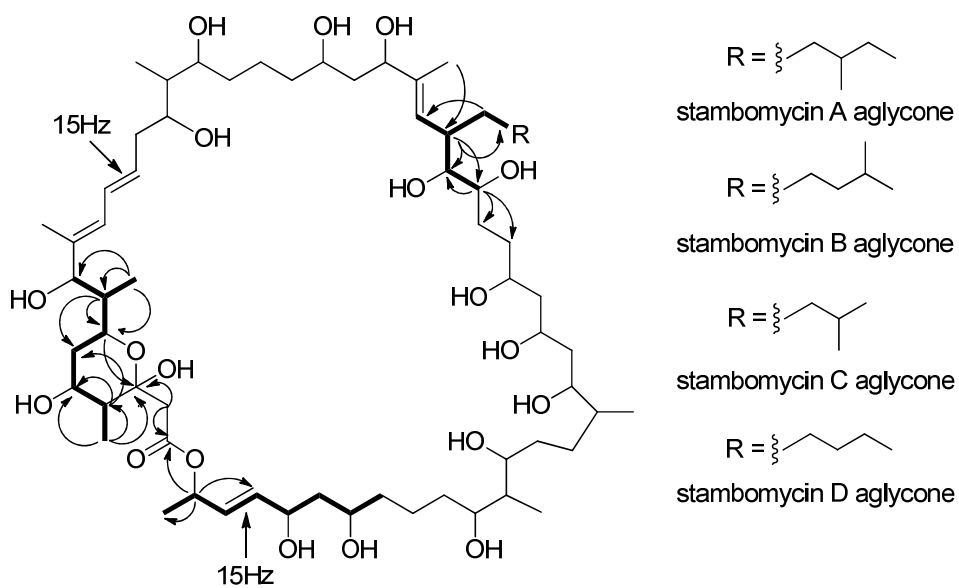


**Fig. S31.** Summary of key COSY (bold lines) HMBC (arrows) and coupling constant data observed for stambomycin aglycones.

**Table S4.** Assignments of  $^1\text{H}$  and  $^{13}\text{C}$  NMR signals for the aglycones of stambomycins A/B. Carbon atom numbering is shown in Fig. S10. Signals for C-1'' to C-7'' of stambomycin B are in brackets.

position	$\delta_{\text{C}}$ (ppm)	$\delta_{\text{H}}$ (ppm)	$J_{\text{H-H}}$ (Hz)
1	173.3		
2	44.2	2.51, 2.75	14.6
3	99.9		
4	47.2	1.36	
4-Me	12.3	1.06	
5	70.1	3.60	
6	39.3	1.45, 1.73	
7	70.1	3.81	
8	40.9	1.60	
8-Me	9.3	0.93	
9	79.6	3.92	7.4
10	136.9		
10-Me	11.9	1.65	
11	127.8	6.05	11.2
12	129.5	6.36	15.1, 11.2
13	131.2	5.79	15.1, 6.8
14	39.8	2.34	6.8
15	75.6	3.78	
16	42.7	1.53	
16-Me	7.4	0.95	
17	75.2	3.72	
18	35.9	1.48	
19	23.3	1.33	
20	38.4	1.47	
21	70.8	3.54	
22	42.9	1.61, 1.67	
23	77.2	4.23	7.3
24	138.7		
24-Me	12.2	1.67	
25	129.6	5.22	10.2
26	41.8	2.45	
1''	32.7 (32.6)	1.19, 1.77 (1.17, 1.81)	
2''	25.4 (26.4)	1.37 (1.36)	
3''	38.1 (32.6)	1.14, 1.29 (1.33)	
4''	35.6 (40.1)	1.30 (1.19, 1.48)	
5''	30.6 (29.6)	1.13 (1.32)	
6''	11.6 (22.9)	0.86 (0.88)	
7''	19.5 (22.9)	0.85 (0.88)	
27	79.4	3.36	
28	73.8	3.48	
29	27.6	1.44, 1.67	
30	35.8	1.45, 1.70	
31	69.6	3.83	
32	46.0	1.50, 1.57	



33	66.6	4.07	
34	41.6	1.48, 1.50	
35	72.5	3.75	
36	41.2	1.48	
36-Me	15.4	0.92	
37	30.4	1.14, 1.29	
38	35.9	1.51	
39	76.1	3.71	
40	42.2	1.51	
40-Me	6.8	0.92	
41	75.6	3.71	
42	33.4	1.43, 1.63	
43	22.7	1.44	
44	38.9	1.45, 1.48	
45	70.5	3.68	
46	44.7	1.59, 1.64	
47	70.9	4.28	6.3, 12.8
48	136.5	5.78	15.0, 6.3
49	130.8	5.73	6.4, 15.0
50	72.9	5.43	6.4,
51	20.6	1.36	6.4

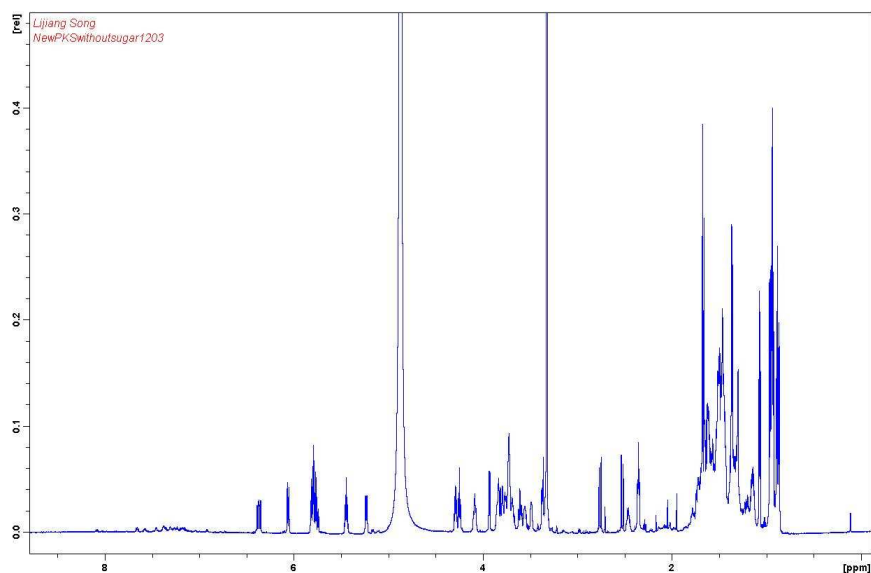


**Fig. S32.**  $^1\text{H}$  NMR spectrum (700 MHz,  $\text{d}_4\text{-MeOH}$ ) of stambomycin A/B aglycones.

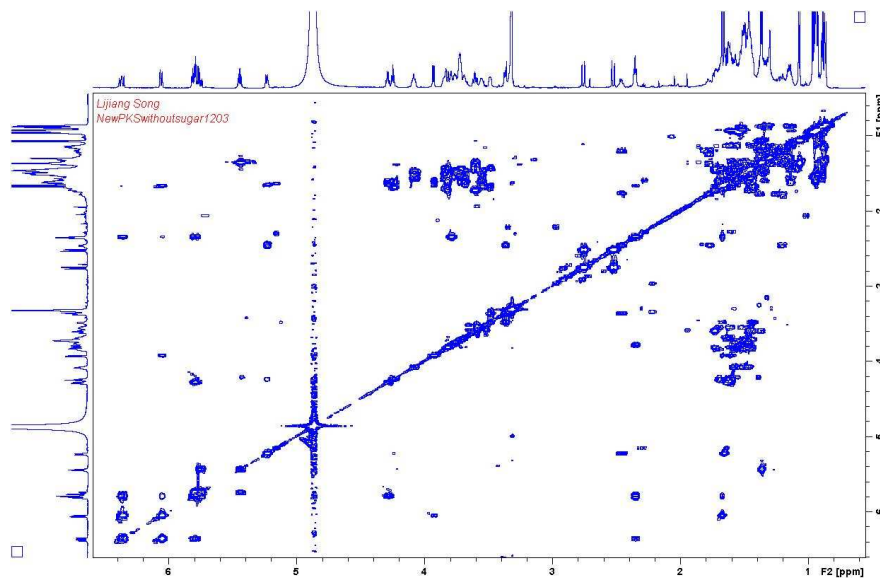


**Fig. S33.** DQFCOSY NMR spectrum (700 MHz,  $d_4$ -MeOH) of stambomycin A/B aglycones.

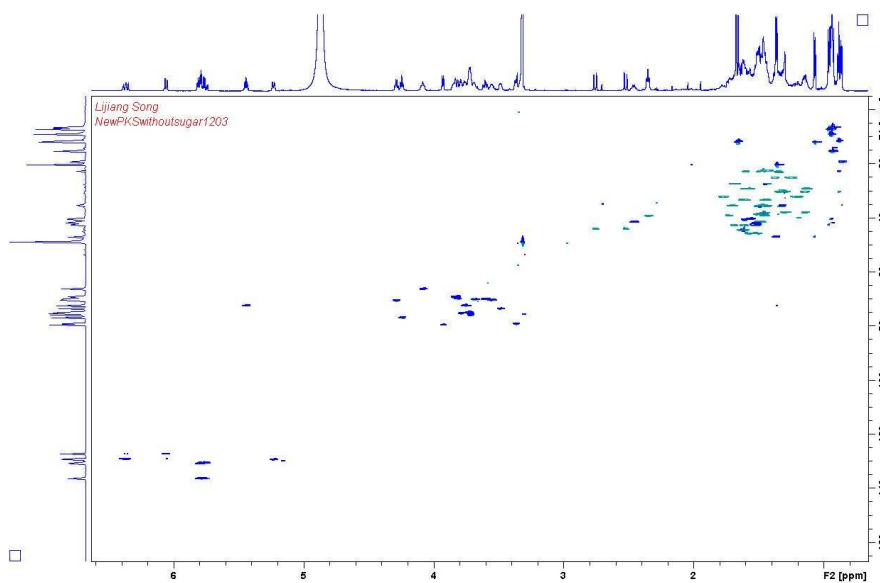


**Fig. S34.** HSQC NMR spectrum (700 MHz/175 MHz,  $d_4$ -MeOH) of stambomycin A/B aglycones.

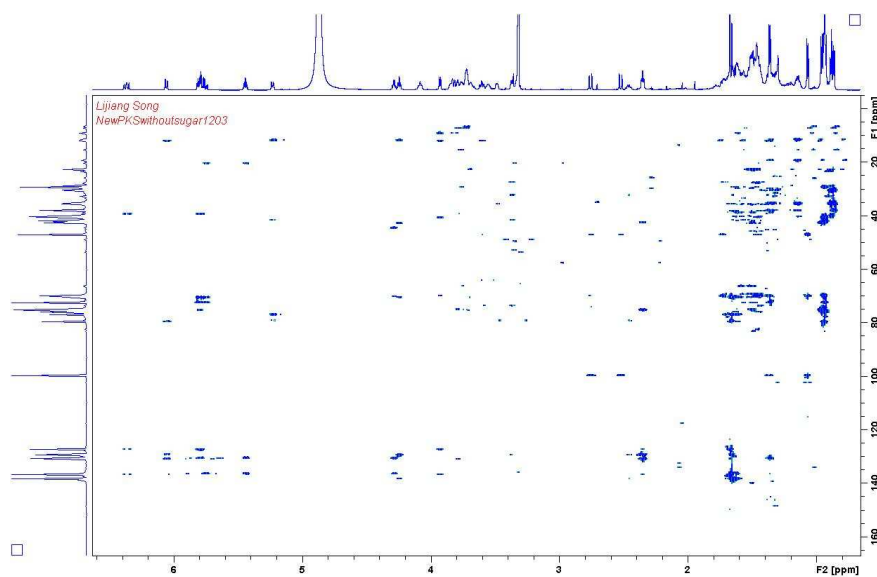


**Fig. S35.** HMBC NMR spectrum (700 MHz/175 MHz, d<sub>4</sub>-MeOH) of stambomycin A/B aglycones.

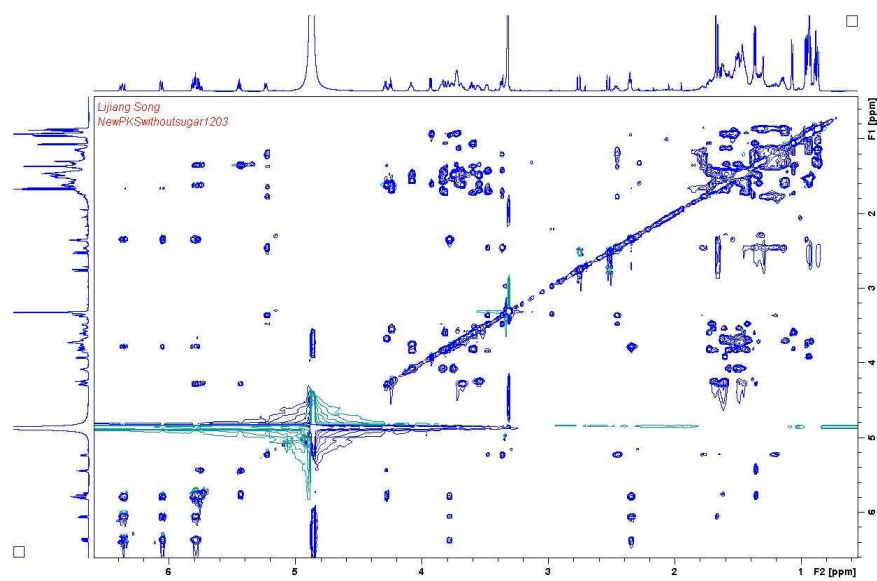


**Fig. S36.** TOCSY NMR spectrum (700 MHz, d<sub>4</sub>-MeOH) of stambomycin A/B aglycones.

**Table S5.** Assignments of  $^1\text{H}$  and  $^{13}\text{C}$  NMR signals for the aglycones of stambomycins C/D. Carbon atom numbering is shown in Fig. S10. Signals for C-1'' to C-6'' of stambomycin D are in brackets.

position	$\delta_{\text{C}}$ (ppm)	$\delta_{\text{H}}$ (ppm)	$J_{\text{H-H}}$ (Hz)
1	172.9		
2	44.2	2.51, 2.75	14.6
3	99.9		
4	47.2	1.36	
4-Me	12.3	1.06	
5	70.1	3.59	
6	39.4	1.45, 1.71	
7	70.0	3.81	
8	40.8	1.61	
8-Me	9.2	0.93	
9	79.6	3.92	7.5
10	136.7		
10-Me	11.9	1.66	
11	127.5	6.05	11.1
12	129.3	6.36	15.0, 11.1
13	131.2	5.79	15.0, 6.8
14	39.6	2.34	6.8
15	75.4	3.78	
16	42.7	1.53	
16-Me	7.3	0.95	
17	75.3	3.72	
18	36.0	1.48	
19	23.1	1.32	
20	38.4	1.45	
21	70.6	3.54	
22	42.8	1.61, 1.67	
23	77.1	4.23	7.3
24	138.6		
24-Me	12.1	1.66	
25	129.4	5.22	10.0
26	41.6	2.44	
1''	32.5 (32.4)	1.19, 1.77 (1.19, 1.80)	
2''	25.6 (27.1)	1.39 (1.41)	
3''	30.6 (32.9)	1.29, 1.29 (1.45)	
4''	40.4 (32.4)	1.21 (1.44)	
5''	22.9 (29.5)	0.88 (1.26)	
6''	22.9 (11.6)	0.88 (0.87)	
27	79.4	3.36	
28	73.7	3.47	
29	27.6	1.44, 1.67	
30	35.7	1.43, 1.71	
31	69.5	3.83	
32	46.0	1.51, 1.57	
33	66.4	4.07	

34	41.6	1.47, 1.51	
35	72.6	3.75	
36	41.6	1.49	
36-Me	15.6	0.93	
37	30.5	1.13, 1.29	
38	35.9	1.50	
39	76.0	3.71	
40	42.1	1.51	
40-Me	6.8	0.91	
41	75.5	3.71	
42	33.4	1.44, 1.62	
43	22.7	1.45	
44	39.1	1.47, 1.51	
45	70.4	3.68	
46	44.7	1.60, 1.63	
47	70.7	4.28	6.4, 12.5
48	136.5	5.78	15.0, 6.4
49	130.7	5.75	6.4, 15.0
50	72.6	5.43	6.4,
51	20.6	1.35	6.4

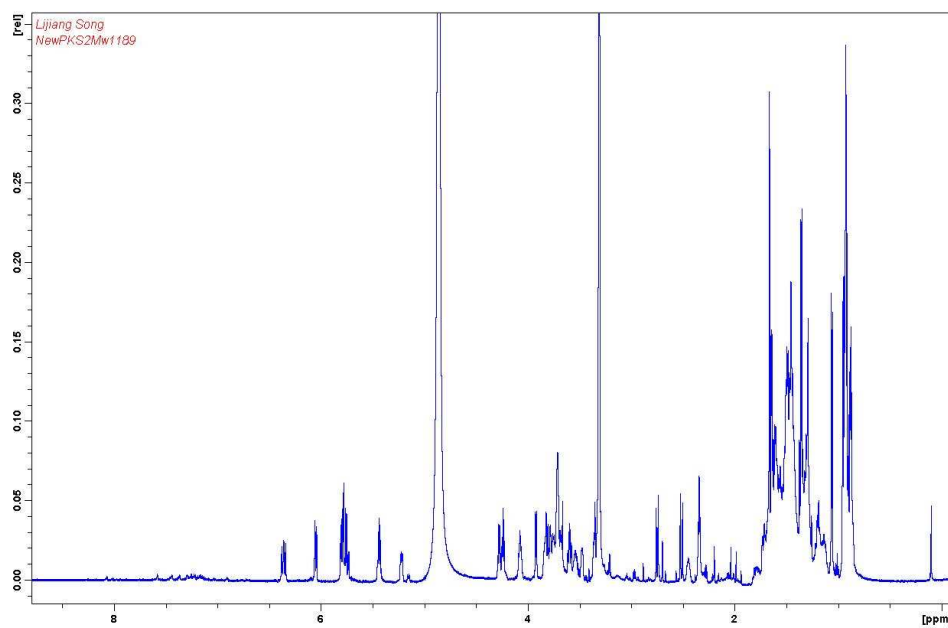


**Fig. S37.**  $^1\text{H}$  NMR spectrum (700 MHz,  $\text{d}_4\text{-MeOH}$ ) of stambomycin C/D aglycones.

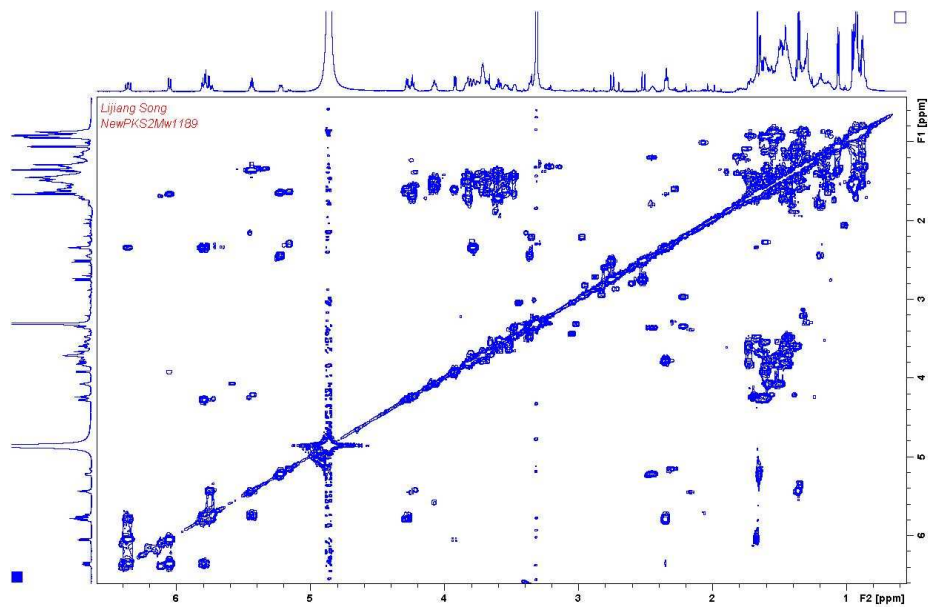


**Fig. S38.** DQFCOSY NMR spectrum (700 MHz, d<sub>4</sub>-MeOH) of stambomycin C/D aglycones.

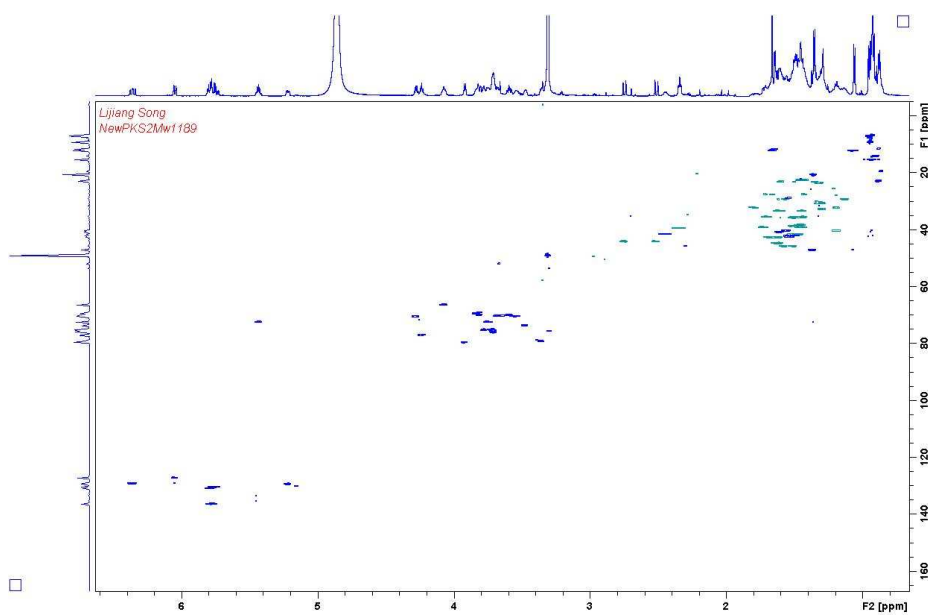


**Fig. S39.** HSQC NMR spectrum (700 MHz/175 MHz, d<sub>4</sub>-MeOH) of stambomycin C/D aglycones.

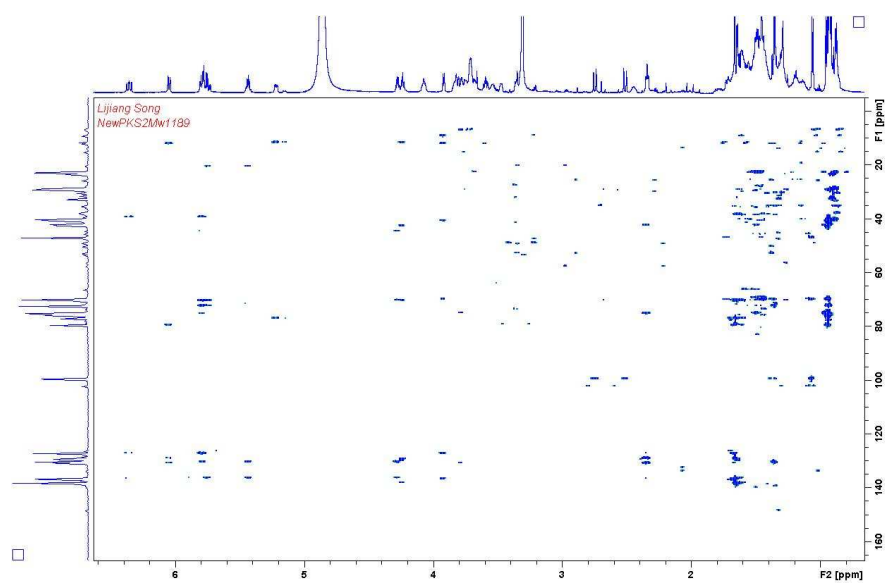


**Fig. S40.** HMBC NMR spectrum (700 MHz/175 MHz, d<sub>4</sub>-MeOH) of stambomycins C/D aglycones.





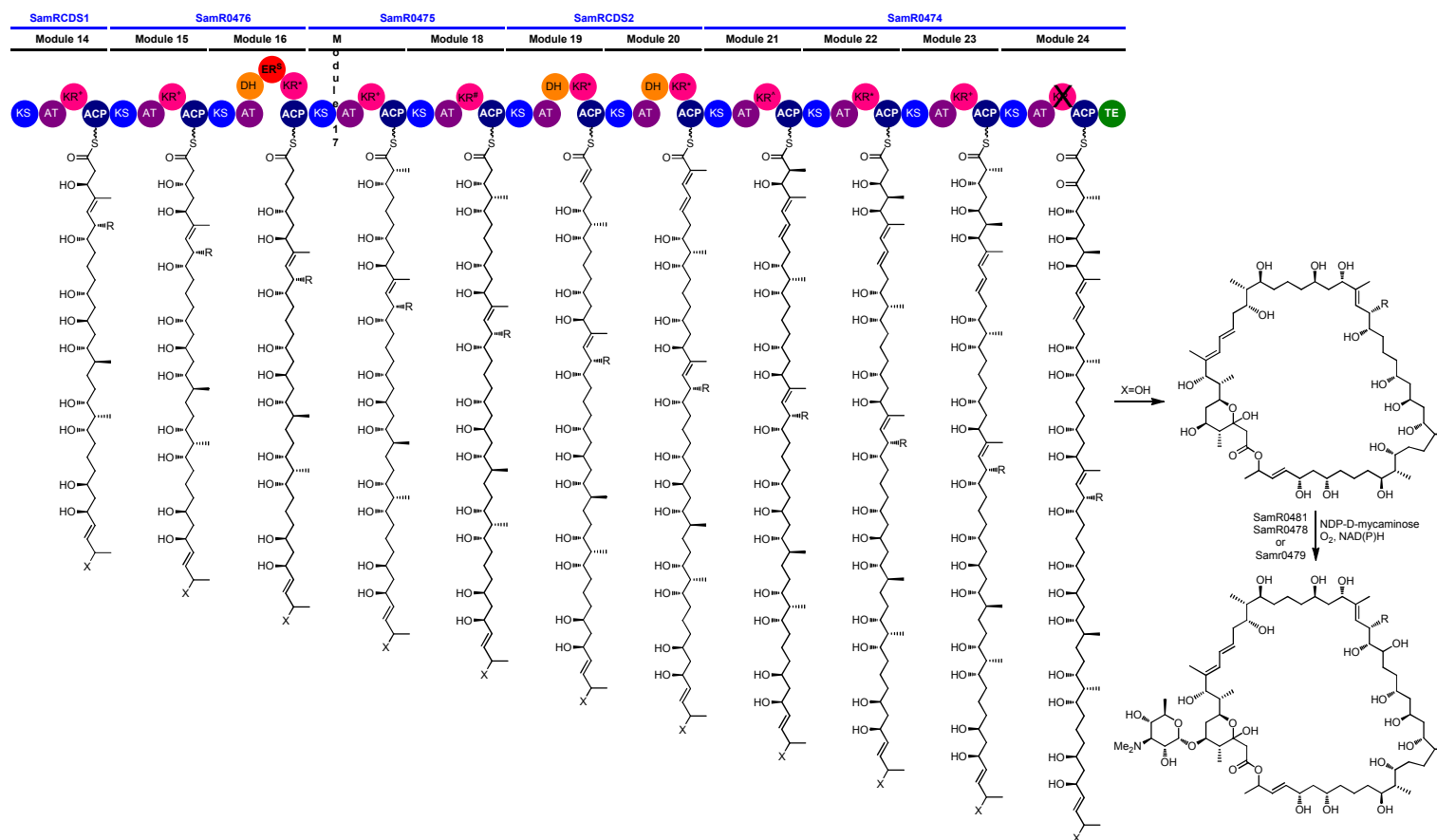


Fig. S41 cont.

Organism	stambomycins		vancomycin	Compounds of reference
	A/B	C/D		
<u>Antibacterial activity (IC<sub>90</sub>, µg/ml):</u>				
<i>Bacillus subtilis</i> BGSC 1A72	ND	33.53 +/- 0.86	0.425+/-0.008	
<i>Enterococcus faecalis</i> LG40	ND	8.65 +/- 0.49	0.970+/-0.003	
<i>Staphylococcus aureus</i> LG21	ND	33.95 +/- 0.16	0.952+/-0.007	
<u>Antiproliferative activity (IC<sub>50</sub>, µM):</u>				
HT29	1.77 +/- 0.04	1.74 +/- 0.04		1.32 +/- 0.08 <sup>a</sup>
H460	1.49 +/- 0.03	1.30 +/- 0.13		1.51 +/- 0.12 <sup>b</sup> ; 5.21 +/- 0.22 <sup>c</sup>
MCF7	>5.34	3.51 +/- 0.16		3.69 +/- 0.11 <sup>d</sup> ; 0.40 +/- 0.03 <sup>e</sup>
PC3	3.39 +/- 0.16	2.79 +/- 0.18		5.64 +/- 0.53 <sup>d</sup> ; 15.44 +/- 0.77 <sup>f</sup>
<u>Cytotoxicity (IC<sub>50</sub>, µM):</u>				
CHO-K1	8.47 +/- 0.67	8.46 +/- 0.52		1.99 +/- 0.25 <sup>a</sup>

**Table S6. Biological activities of stambomycins A/B and C/D.** IC<sub>90</sub> and IC<sub>50</sub> indicate the concentrations needed to inhibit the growth of 90% and 50% of cells in the population, respectively. HT29: human colon adenocarcinoma cell line; H460: lung cancer cell line; MCF7: breast cancer cell line; PC3: prostate cancer cell line; CHO-K1: adult Chinese hamster ovary sane cell line. ND: the IC<sub>90</sub> values for stambomycins A/B were not determined, but these compounds were shown to possess antibacterial activity. Vancomycin was used as positive control in the antibacterial assays. The compounds used as reference for antiproliferative activity or cytotoxicity tests are doxorubicin<sup>a</sup> for HT29 and CHO-K1, mycophenolic acid<sup>b</sup> and 5-fluorouracyl<sup>c</sup> for H460, mitoxantrone<sup>d</sup> and CD437<sup>e</sup> for MCF7 and mitoxantrone and vinorelbin<sup>f</sup> for PC3.

Species	Protein	Function	Reference
<i>S. venezuelae</i>	PikD*	Pikromycin biosynthesis	(11)
<i>S. hygroscopicus</i>	RapH*	Rapamycin biosynthesis	(12)
<i>S. hygroscopicus</i>	Orf6	Type I PKS cluster	(13)
<i>S. noursei</i>	NysRI, NysRII, NysRIII*	Nystatin biosynthesis	(14)
<i>S. cinnamomensis</i>	MonH	Monensis biosynthesis	(15)
<i>S. avermitilis</i>	AveR*	Avermectin biosynthesis	(16)
<i>Streptomyces</i> sp. CK4412	TmcN*	Tautomycetin biosynthesis	(17)
<i>S. albus</i>	SalRI, SalRII	Salinomycin biosynthesis	(18)
<i>S. natalensis</i>	PimR*	Pimaricin biosynthesis	(19)
<i>S. hygroscopicus</i> 17997	GdmRI, GdmRII*	Geldanamycin biosynthesis	(20)
<i>S. hygroscopicus</i> var.	FkbN	FK520 biosynthesis	(21)
<i>Streptomyces</i> sp. FR-008	FscRII, FscRIII, FscRIV	FR-008/candicidin	(22)
<i>S. nodosus</i>	AmphRI, AmphRII,	Amphotericin biosynthesis	(23)
<i>S. platensis</i> Mer-11107	PldR	Pladienolide biosynthesis	(24)
<i>S. ambofaciens</i>	SAMR0484*	Stambomycin biosynthesis	This work
<i>S. narbonensis</i>	NbmM	Narbomycin biosynthesis	AAM88362.1
<i>S. avermitilis</i>	OlmRII, OlmRI	Oligomycin biosynthesis	(25)
<i>Streptomyces</i> sp307-9	TamH <sup>#</sup>	Tirandamycin biosynthesis	(26)
<i>S. nanchangensis</i>	NlmRI	Type I PKS cluster	AAS46340.1
<i>S. aizunensis</i>	Orf30	ECO-02301 biosynthesis	(27)
<i>S. nanchangensis</i>	MeiR	Meilingmycin biosynthesis	(28)
<i>S. sp</i> MP39-85	MlaH	ML-449 biosynthesis	(29)
<i>Streptomyces</i> sp	BecH	BE-14106 biosynthesis	(30)
<i>Nonomuraea</i>	Dbv3	A40926 biosynthesis	(31)
<i>S. hygroscopicus</i>	HbmRII, HbmRI	Herbimycin biosynthesis	(32)
<i>S. lydicus</i>	SlgR2 <sup>#</sup>	Streptolydigin biosynthesis	(33)
<i>S. neyagawaensis</i>	Orf3	Concanamycin A	(34)
<i>Amycolatopsis orientalis</i>	Orf4	ECO-0501 biosynthesis	(35)
<i>S. carzinostaticus</i>	Orf2	Neocarzilin biosynthesis	(36)
<i>S. griseus</i>	Sgr6177	Type I PKS cluster	(37)
<i>S. cyaneogriseus</i>	NemR	Nemadectin biosynthesis	BAF85834.1
<i>S. hygroscopicus</i>	FkbN	FK520 biosynthesis	(21)
<i>S. antibioticus</i>	IdmG	Indanomycin biosynthesis	(38)
<i>S. lasaliensis</i>	Lsd8	Lasalocid biosynthesis	(39)

**Table S7.** List of 44 LAL proteins from actinomycetes species found in literature involved in known secondary metabolite biosynthesis (of modular PKS). \*LAL regulators that have been characterized experimentally. <sup>#</sup>LAL regulators of PKS/NRPS clusters.

Species	Genes
<i>S. albus</i> J1074	fscRII, fscRIII, fscRIV
<i>S. roseosporus</i> NRRL 15998	SSGG_00417; SSGG_05502
<i>S. hygrosopicus</i> ATCC 53653	SSOG_00531; SSOG_00533; SSOG_05729; SSOG_07879
<i>Micromonospora carbonacea</i> ATCC 39149	MCAG_00565; MCAG_05134
<i>Streptomyces</i> sp. AA4	SSMG_05933
<i>S. clavuligerus</i> ATCC 27064	SSCG_03496
<i>Streptomyces</i> sp. C	SSNG_07480
<i>S. viridochromogenes</i> DSM 40736	SSQG_00945; SSQG_00966
<i>Kutzneria</i> sp. 744	KUTG_07746; KUTG_08953; KUTG_09296
<i>S. roseosporus</i> NRRL 11379 (v4)	SSIG_05739
<i>Micromonospora</i> sp. M42	MCBG_00014; MCBG_00015
<i>Streptomyces</i> sp. Mg1	SSAG_08104
<i>Streptomyces</i> sp. E14	SSTG_03938

**Table S8.** List of putative LAL regulatory genes involved in the regulation of a secondary metabolite gene cluster. The Blastp analysis was obtained using SamR0484 as bait and using the actinomycetes genome database of the Broad Institute

([http://www.broadinstitute.org/annotation/genome/streptomyces\\_group/MultiHome.html](http://www.broadinstitute.org/annotation/genome/streptomyces_group/MultiHome.html)). The genes retained were found nearside a modular PKS (except for SSTG\_03938 located within a hybrid PKS-NRPS cluster) and the encoding proteins contain the typical domains of a LAL regulator.

Strains, BAC or plasmid	Principal characteristics <sup>a</sup>	Reference
<b>Strains:</b>		
<i>S. ambofaciens</i>		
ATCC23877	wildtype	(40)
ATCC/pIB139	empty vector integrated in the <i>attB</i> site	This work
ATCC/OE484	Overexpression of the LAL regulator	This work
ATCC/OE468-9	Overexpression of the two component system	This work
ATCC/OE484/Δ467	Overexpression of the LAL regulator and the gene <i>samR0467</i> replaced by a kanamycin resistance cassette	This work
ATCC/OE484/Δ481	Overexpression of the LAL regulator and the gene <i>samR0481</i> replaced by an apramycin resistance cassette	This work
<i>E. coli</i>		
DH5α	General cloning strain	(41)
ET12567/pUZ8002	Nonmethylating strain with mobilization plasmid for conjugation with <i>Streptomyces</i>	(42)
BW25113/pKD20	Strain used for the PCR-targeting mutagenesis ( <i>gam</i> , <i>bet</i> , <i>exo</i> , <i>bla</i> )	(43)
<b>BAC or plasmids:</b>		
BBB	BAC from the genomic library of <i>S. ambofaciens</i> ( <i>cat</i> )	(44)
BBC	BAC from the genomic library of <i>S. ambofaciens</i> ( <i>cat</i> )	(44)
BBB/Δ467::neo+oriT	<i>samR0467</i> replaced by a neomycin cassette in BBB ( <i>cat</i> , <i>neo</i> )	This work
BBBspec/Δ467::neo+oriT	<i>cat</i> of BBB/Δ467::neo+oriT replaced by a <i>aadA</i> cassette	This work
BBC/Δ481::aac(3)IV+oriT	<i>samR0481</i> replaced by an apramycin cassette in BBC ( <i>cat</i> , <i>neo</i> )	This work
BBCspec/Δ481::aac(3)IV+oriT	<i>cat</i> BBC/Δ481::aac(3)IV+oriT replaced by a <i>aadA</i> cassette	This work
pIJ776	<i>oriT</i> , <i>neo</i>	(45)
pIJ778	<i>oriT</i> , <i>aadA</i>	(45)
pGEMT-easy	PCR cloning vector, <i>bla</i>	Promega
pGEMT-0484	pGEMTeasy + <i>samR0484</i> without promoter region	This work
pIB139	Conjugative and integrative plasmid ( <i>oriT attP<sub>φC31</sub> int<sub>φC31</sub> aac(3)IV ermEp*</i> )	(46)
pOE-0484	pIB139 + <i>samR0484</i>	This work
pOE-4689	pIB139 + <i>samR0468-9</i>	This work

**Table S9.** List of strains, plasmids and BACs used in this work. <sup>a</sup> *bla*, ampicillin resistance gene; *neo*, kanamycin resistance gene; *aac(3)IV*, apramycin resistance gene; *oriT*, origin of transfer; *aadA*, spectinomycin/streptomycin resistance gene; *gam*, inhibitor of the host exonuclease V; *bet*, single-stranded DNA binding protein; *exo*, exonuclease promoting recombination along with *bet*; *cat*, chloramphenicol resistance gene; *attP<sub>φC31</sub>*, *φC31* attachment site from the *φC31* phage; *int<sub>φC31</sub>*, integrase gene of *φC31*.

Primers	Nucleotide sequence (5'→3')
Overexpression:	
OE484-F	<u>CATATGCTGGTCCATCGAGACGAAC</u>
OE484-R	<u>TCTAGACTCTGCTCTCTCCAAGGCT</u>
OE468-F	<u>AGGTCTAGAGTCAGCCGAGGAAAC</u>
OE469-R	<u>CATATGACGAACGTGTCACGCGCGC</u>
Deletion:	
D467-F	<b>GGCGATCTCGCGCCGTCAAGTGATTT</b> CGGGGCATTCATGTGTAGGCTGGAGCTGCTTC
D467-R	<b>CAGAGCGACTCCCAGCGGGCAGGACCGTACATGGCGTCA</b> ATTCGGGGATCCGTCGACC
D481-F	<b>GGCGGGCTCCGGGCCGCGGGGCCGACCC</b> TCCCGTCTGCCTCTTCGTCCCGAAGCA
D481-R	<b>ACTGTTTCCGTCGCGGGCCCGCCTGGAGGACGACA</b> ATGGCGCGCGCTTCGTTCCGGGAC
Transcriptional analysis:	
RT-467-F	GTCGCCGATCACCAGGAA
RT-467-R	AGGTCGCGGAACGCCTTGTC
RT-465-F	TGCCTGCGGTGCTCCACCAA
RT-465-R	CGTCGTCTTCTCCTCCATCG
RT-477-F	GGAACAGCTCGCCGTACTCC
RT-477-R	CCGAACTCGTCGGCGTATGG
RT-474-F	ACCGCGCCGAGGTGAGACA
RT-474-R	GCTGCTCGCCTGCGTGGACA
RT-484-F	CTGGAGACCTTCGGGGAGTG
RT-484-R	TGCCCAGCACTCCGAAATG
RT-468-F	GTGGGTCAGGTGCGTCTTGAC
RT-468-R	ACTGCAAGTGCTGGAGCACG
RT-469-F	GAGGACGGGAGGGCTGAAGC
RT-469-R	GCGTGGCATCCGACGCGACCC
HrdB-F	CGCGGCATGCTCTTCCT
HrdB-R	AGGTGGCGTACGTGGAGAAC

**Table S10.** Oligonucleotide primers used in this work. The underlined nucleotides are *NdeI* and *XbaI* restriction sites. The bold nucleotides are identical to the sequences at the extremities of the *samR0467* (D467-F, -R) and *samR0481* (D481-F, -R) genes, which were deleted.

## References

1. Kieser T, Bibb MJ, Buttner MJ, Chater KF, & Hopwood DA (2000) Practical *Streptomyces* genetics. *John Innes Foundation, Norwich, United Kingdom*.
2. Pernodet JL, Alegre MT, Blondelet-Rouault MH, & Guerineau M (1993) Resistance to spiramycin in *Streptomyces ambofaciens*, the producer organism, involves at least two different mechanisms. *J Gen Microbiol* 139(5):1003-1011.
3. Sambrook J, Fritsch EF, & Maniatis T (1989) Molecular cloning: a laboratory manual, 2nd ed. *Cold Spring Harbor Laboratory Press, Cold Spring Harbor, N.Y.*
4. Leblond P, *et al.* (1996) The unstable region of *Streptomyces ambofaciens* includes 210 kb terminal inverted repeats flanking the extremities of the linear chromosomal DNA. *Mol Microbiol* 19(2):261-271.
5. Pang X, *et al.* (2004) Functional angucycline-like antibiotic gene cluster in the terminal inverted repeats of the *Streptomyces ambofaciens* linear chromosome. *Antimicrob Agents Chemother* 48(2):575-588.
6. Yadav G, Gokhale RS, & Mohanty D (2003) Computational approach for prediction of domain organization and substrate specificity of modular polyketide synthases. *J Mol Biol* 328(2):335-363.
7. Aparicio JF, *et al.* (1996) Organization of the biosynthetic gene cluster for rapamycin in *Streptomyces hygroscopicus*: analysis of the enzymatic domains in the modular polyketide synthase. *Gene* 169(1):9-16.
8. Keatinge-Clay AT (2007) A tylosin ketoreductase reveals how chirality is determined in polyketides. *Chem Biol* 14(8):898-908.
9. Kwan DH, *et al.* (2008) Prediction and manipulation of the stereochemistry of enoylreduction in modular polyketide synthases. *Chem Biol* 15(11):1231-1240.
10. Karray F, *et al.* (2007) Organization of the biosynthetic gene cluster for the macrolide antibiotic spiramycin in *Streptomyces ambofaciens*. *Microbiology* 153(Pt 12):4111-4122.
11. Wilson DJ, Xue Y, Reynolds KA, & Sherman DH (2001) Characterization and analysis of the PikD regulatory factor in the pikromycin biosynthetic pathway of *Streptomyces venezuelae*. *J Bacteriol* 183(11):3468-3475.
12. Kuscer E, *et al.* (2007) Roles of *rapH* and *rapG* in positive regulation of rapamycin biosynthesis in *Streptomyces hygroscopicus*. *J Bacteriol* 189(13):4756-4763.
13. Ruan X, Stassi D, Lax SA, & Katz L (1997) A second type-I PKS gene cluster isolated from *Streptomyces hygroscopicus* ATCC 29253, a rapamycin-producing strain. *Gene* 203(1):1-9.
14. Sekurova ON, *et al.* (2004) In vivo analysis of the regulatory genes in the nystatin biosynthetic gene cluster of *Streptomyces noursei* ATCC 11455 reveals their differential control over antibiotic biosynthesis. *J Bacteriol* 186(5):1345-1354.
15. Oliynyk M, *et al.* (2003) Analysis of the biosynthetic gene cluster for the polyether antibiotic monensin in *Streptomyces cinnamonensis* and evidence for the role of *monB* and *monC* genes in oxidative cyclization. *Mol Microbiol* 49(5):1179-1190.
16. Kitani S, Ikeda H, Sakamoto T, Noguchi S, & Nihira T (2009) Characterization of a regulatory gene, *aveR*, for the biosynthesis of avermectin in *Streptomyces avermitilis*. *Appl Microbiol Biotechnol* 82(6):1089-1096.

17. Hur YA, Choi SS, Sherman DH, & Kim ES (2008) Identification of TmcN as a pathway-specific positive regulator of tautomycin biosynthesis in *Streptomyces sp.* CK4412. *Microbiology* 154(Pt 10):2912-2919.
18. Knirschova R, *et al.* (2007) Multiple regulatory genes in the salinomycin biosynthetic gene cluster of *Streptomyces albus* CCM 4719. *Folia Microbiol (Praha)* 52(4):359-365.
19. Anton N, Mendes MV, Martin JF, & Aparicio JF (2004) Identification of PimR as a positive regulator of pimarin biosynthesis in *Streptomyces natalensis*. *J Bacteriol* 186(9):2567-2575.
20. He W, Lei J, Liu Y, & Wang Y (2008) The LuxR family members GdmRI and GdmRII are positive regulators of geldanamycin biosynthesis in *Streptomyces hygroscopicus* 17997. *Arch Microbiol* 189(5):501-510.
21. Wu K, Chung L, Revill WP, Katz L, & Reeves CD (2000) The FK520 gene cluster of *Streptomyces hygroscopicus* var. *ascohyeticus* (ATCC 14891) contains genes for biosynthesis of unusual polyketide extender units. *Gene* 251(1):81-90.
22. Chen S, *et al.* (2003) Organizational and mutational analysis of a complete FR-008/candicidin gene cluster encoding a structurally related polyene complex. *Chem Biol* 10(11):1065-1076.
23. Carmody M, *et al.* (2004) Analysis and manipulation of amphotericin biosynthetic genes by means of modified phage KC515 transduction techniques. *Gene* 343(1):107-115.
24. Machida K, *et al.* (2008) Organization of the biosynthetic gene cluster for the polyketide antitumor macrolide, pladienolide, in *Streptomyces platensis* Mer-11107. *Biosci Biotechnol Biochem* 72(11):2946-2952.
25. Guo J, *et al.* (2010) The pathway-specific regulator AveR from *Streptomyces avermitilis* positively regulates avermectin production while it negatively affects oligomycin biosynthesis. *Mol Genet Genomics* 283(2):123-133.
26. Carlson JC, *et al.* (2010) Identification of the tirandamycin biosynthetic gene cluster from *Streptomyces sp.* 307-9. *Chembiochem* 11(4):564-572.
27. McAlpine JB, *et al.* (2005) Microbial genomics as a guide to drug discovery and structural elucidation: ECO-02301, a novel antifungal agent, as an example. *J Nat Prod* 68(4):493-496.
28. Sun Y, Zhou X, Tu G, & Deng Z (2003) Identification of a gene cluster encoding meilingmycin biosynthesis among multiple polyketide synthase contigs isolated from *Streptomyces nanchangensis* NS3226. *Arch Microbiol* 180(2):101-107.
29. Jorgensen H, *et al.* (2010) Insights into the evolution of macrolactam biosynthesis through cloning and comparative analysis of the biosynthetic gene cluster for a novel macrocyclic lactam, ML-449. *Appl Environ Microbiol* 76(1):283-293.
30. Jorgensen H, *et al.* (2009) Biosynthesis of macrolactam BE-14106 involves two distinct PKS systems and amino acid processing enzymes for generation of the aminoacyl starter unit. *Chem Biol* 16(10):1109-1121.
31. Sosio M, Stinchi S, Beltrametti F, Lazzarini A, & Donadio S (2003) The gene cluster for the biosynthesis of the glycopeptide antibiotic A40926 by *nonomuraea* species. *Chem Biol* 10(6):541-549.



32. Rascher A, Hu Z, Buchanan GO, Reid R, & Hutchinson CR (2005) Insights into the biosynthesis of the benzoquinone ansamycins geldanamycin and herbimycin, obtained by gene sequencing and disruption. *Appl Environ Microbiol* 71(8):4862-4871.
33. Olano C, *et al.* (2009) Deciphering biosynthesis of the RNA polymerase inhibitor streptolydigin and generation of glycosylated derivatives. *Chem Biol* 16(10):1031-1044.
34. Haydock SF, *et al.* (2005) Organization of the biosynthetic gene cluster for the macrolide concanamycin A in *Streptomyces neyagawaensis* ATCC 27449. *Microbiology* 151(Pt 10):3161-3169.
35. Banskota AH, *et al.* (2006) Genomic analyses lead to novel secondary metabolites. Part 3. ECO-0501, a novel antibacterial of a new class. *J Antibiot (Tokyo)* 59(9):533-542.
36. Otsuka M, Ichinose K, Fujii I, & Ebizuka Y (2004) Cloning, sequencing, and functional analysis of an iterative type I polyketide synthase gene cluster for biosynthesis of the antitumor chlorinated polyenone neocarzilin in "*Streptomyces carzinostaticus*". *Antimicrob Agents Chemother* 48(9):3468-3476.
37. Ohnishi Y, *et al.* (2008) Genome sequence of the streptomycin-producing microorganism *Streptomyces griseus* IFO 13350. *J Bacteriol* 190(11):4050-4060.
38. Li C, Roeger KE, & Kelly WL (2009) Analysis of the indanomycin biosynthetic gene cluster from *Streptomyces antibioticus* NRRL 8167. *Chembiochem* 10(6):1064-1072.
39. Migita A, *et al.* (2009) Identification of a gene cluster of polyether antibiotic lasalocid from *Streptomyces lasaliensis*. *Biosci Biotechnol Biochem* 73(1):169-176.
40. Pinnert-Sindico S (1954) Une nouvelle espèce de *Streptomyces* productrice d'antibiotiques : *Streptomyces ambofaciens* n. sp. caractères culturaux. [A new species of *Streptomyces* productive of antibiotics: *Streptomyces ambofaciens*. Culture characteristics]. *Ann Inst Pasteur (Paris)* 87(6):702-707.
41. Hanahan D (1983) Studies on transformation of *Escherichia coli* with plasmids. *Journal of Molecular Biology* 166:557-580.
42. MacNeil DJ, *et al.* (1992) Analysis of *Streptomyces avermitilis* genes required for avermectin biosynthesis utilizing a novel integration vector. *Gene* 111(1):61-68.
43. Datsenko KA & Wanner BL (2000) One-step inactivation of chromosomal genes in *Escherichia coli* K-12 using PCR products. *Proc Natl Acad Sci U S A* 97(12):6640-6645.
44. Choulet F, *et al.* (2006) Evolution of the terminal regions of the *Streptomyces* linear chromosome. *Mol Biol Evol* 23(12):2361-2369.
45. Gust B, Challis GL, Fowler K, Kieser T, & Chater KF (2003) PCR-targeted *Streptomyces* gene replacement identifies a protein domain needed for biosynthesis of the sesquiterpene soil odor geosmin. *Proc Natl Acad Sci U S A* 100(4):1541-1546.
46. Wilkinson CJ, *et al.* (2002) Increasing the efficiency of heterologous promoters in actinomycetes. *J Mol Microbiol Biotechnol* 4(4):417-426.